MICROBIOLOGY

Splenic red pulp macrophages eliminate the liver-resistant *Streptococcus pneumoniae* from the blood circulation of mice

Haoran An[1,2,3]*†, Yijia Huang[4]†, Zhifeng Zhao[5]†, Kunpeng Li[3], Jingjing Meng[1], Xueting Huang[3], Xianbin Tian[3], Hongyu Zhou[5], Jiamin Wu[5], Qionghai Dai[5]*, Jing-Ren Zhang[3]*

Invasive infections by encapsulated bacteria are the major cause of human morbidity and mortality. The liver resident macrophages, Kupffer cells, form the hepatic firewall to clear many encapsulated bacteria in the blood circulation but fail to control certain high-virulence capsule types. Here we report that the spleen is the backup immune organ to clear the liver-resistant serotypes of *Streptococcus pneumoniae* (pneumococcus), a leading human pathogen. Asplenic mice failed to control the growth of the liver-resistant pneumococci in the blood circulation. Immunologic and genetic analyses identified splenic red pulp (RP) macrophages as the major phagocytes for bacterial clearance. Furthermore, the plasma natural antibodies against the cell wall phosphocholine and the complement system were necessary for RP macrophage–mediated immunity. These findings have provided a conceptual framework for the innate defense against blood bacterial infections, a mechanistic explanation for the hyper-susceptibility of asplenic individuals to *S. pneumoniae*, and a proof of concept for developing vaccines and therapeutic antibodies against encapsulated pathogens.

INTRODUCTION

Encapsulated bacteria are the major cause of invasive bacterial diseases in humans, such as pneumonia, sepsis, and meningitis (*1*, *2*). Capsules are the outermost structures of many bacteria and known to be essential for the survival and virulence of invasive bacteria. Capsules are well known for their antiphagocytic properties owing to certain physical characteristics of the capsules (e.g., hyperviscosity and negative charge) (*3*–*5*). Virtually all the capsules are composed of capsular polysaccharides (CPSs) (*2*, *6*). Many pathogenic bacteria produce large numbers of capsular variants or serotypes with substantial differences in structure and antigenicity (*2*). More than 100 capsular serotypes have been reported in *Streptococcus pneumoniae* (*7*). Capsular types are clinically linked to disease potentials of encapsulated bacteria.

The liver and spleen are responsible for the removal of invading bacteria and other foreign particles from the blood circulation since intravenously administrated vital stains and bacteria are trapped in the liver and spleen of mammals (*8*–*11*), which has led to the loosely defined concept of the "reticuloendothelial system" (*12*, *13*). In the recent decades, the liver has been shown as the major organ to trap acapsular bacteria or the vascular "firewall" against invading bacteria in the bloodstream (*14*, *15*). The liver resident macrophage Kupffer cells (KCs) execute the immune/scavenging function (*16*). Our recent works have shown that KCs also capture and kill many encapsulated bacteria in the bloodstream of mice (referred to as the low-virulence or liver-susceptible capsule types), but certain high-virulence (or liver-resistant) capsule types are able to escape the KC recognition (*17*, *18*).

The spleen, the largest immune organ in the body, is well-known for its defense against encapsulated bacteria (*19*, *20*). Individuals with asplenia (the congenital or acquired absence of the spleen) are highly susceptible to overwhelming infections by several encapsulated bacteria, with an approximately 50-fold higher risk of developing severe septic infections and a mortality rate of 50 to 70% (*21*, *22*). *S. pneumoniae* is the most common causal organism associated with 50 to 90% of postsplenectomy infection cases, with *Haemophilus influenzae* and *Neisseria meningitidis* as the less frequent pathogens (*23*). These bacteria, although distantly related at the evolutionary scale, are all covered by variable polysaccharide capsules. The specific reason for the critical role of spleen in defense against these bacteria remains unclear.

The spleen is a highly compartmentalized organ with three functionally interrelated compartments: red pulp (RP), white pulp (WP), and marginal zone (MZ) (*20*, *24*). The sponge-like RP is filled with slow-flowing blood from sinuses and cords, which is important for blood filtering by RP macrophages. The WP contains B and T lymphocytes for the maturation of B cells and antibody production. The MZ is located at the extreme periphery of the WP and contains natural antibody (nAb)–producing B cells, MZ macrophages, and metallophilic (MP) macrophages. Besides, neutrophils and monocytes are abundantly present in the spleen (*25*, *26*). Despite the well-recognized importance of the spleen in defending against circulating bacteria, the precise immune mechanisms remain largely speculative. RP macrophages have been shown to capture blood-borne pneumococci but lack phagocytic killing capabilities; instead, they rely on neutrophils to kill the immobilized bacteria (*25*). Conversely, a separate study has reported that RP macrophages are predominantly responsible for splenic killing of *S. pneumoniae*; neutrophils and dendritic cells are dispensable (*27*). MZ macrophages have been described to engage pneumococcal capsules via the lectin receptor SIGN-R1 (*28*, *29*), contributing to host immunity to pneumococcal disease (*30*, *31*). MP macrophages seem to play an opposite role by serving as an intracellular replication site for pneumococci (*32*). Furthermore, nAbs produced by MZ B cells are implicated

[1]Institute of Medical Technology, Peking University Health Science Center, Beijing 100191, China. [2]Department of Microbiology and Infectious Disease Center, Peking University Health Science Center, Beijing 100191, China. [3]Center for Infectious Biology, School of Basic Medical Sciences, Tsinghua University, Beijing 100084, China. [4]Department of Parasitology, School of Basic Medical Sciences, Wenzhou Medical University, Wenzhou, Zhejiang 325035, China. [5]Department of Automation, Tsinghua University, Beijing 100084, China.
*Corresponding author. Email: ahr@bjmu.edu.cn (H.A.); daiqh@tsinghua.edu.cn (Q.D.); zhanglab@tsinghua.edu.cn (J.-R.Z.)
†These authors contributed equally to this work.

in the opsonophagocytosis of *S. pneumoniae*, *H. influenzae*, and *N. meningitidis* (*33*). Despite these insights, the integration of the cellular and molecular effectors in orchestrating the splenic innate defense against encapsulated pathogens remains poorly understood.

The current literature has demonstrated the importance of both the spleen and liver in host defense against bacterial infections, but it remains largely unknown how the spleen and liver divide the labor in the clearance of invading bacteria mainly due to the lack of appropriate tools in dissecting the functional redundancy. This study takes advantage of the liver-resistant and -susceptible capsular types to define the specific contribution of the spleen to the clearance of encapsulated bacteria based on our previous studies (*17*, *18*). We found that the spleen clears the liver-resistant pneumococci via the orchestrated actions of RP macrophages, nAbs, and the complement system.

RESULTS

Spleen eliminates the liver-resistant high-virulence *S. pneumoniae*

Our previous studies have shown that the liver-resistant high-virulence (HV) serotypes of pneumococci circumvent phagocytic capture and clearance of KCs in the liver vasculatures, leading to overwhelming septicemia and death (*17*). During that study, we noticed slow but substantial elimination of the liver-resistant pneumococci from the bloodstream of mice in the first 12 hours post intravenous infection, so called "eclipse" phase (*34*), although bacteremia relapsed to a lethal stage at the later phase of infection (Fig. 1A, *Spn*6A). In sharp contrast, liver-susceptible low-virulence (LV) serotypes were rapidly eradicated regardless of the clinical isolate or isogenic capsule–switched strain (Fig. 1A, *Spn*14, and fig. S1, A to C). To determine the extent of this anti-HV pneumococcal immunity, we performed similar infection with lower doses of *Spn*6A [10^3 to 10^5 colony-forming units (CFUs)] and monitored the bacteremia kinetics (Fig. 1B) and survival (Fig. 1C). Although all the mice infected with four doses showed substantial clearance of blood-borne bacteria at 12 hours, those receiving relatively higher doses displayed higher levels of bacteremia. There were undetectable blood bacteria in the group of 10^3 CFU; mice infected with 10^4 to 10^6 CFU exhibited increasing levels of bacteremia that were proportional to the inoculum doses (Fig. 1B). While infection with 10^4 CFU led to a mild bacteremia of 1300 CFU at 12 hours, relatively higher levels of bacteremia were observed in groups of 10^5 CFU (4500 CFU/ml) and 10^6 CFU (4700 CFU/ml). Consistently, there were undetectable bacteria in mice infected with 10^3 and 10^4 CFU at 48 hours, and substantial levels of bacteria were present in the blood circulation of

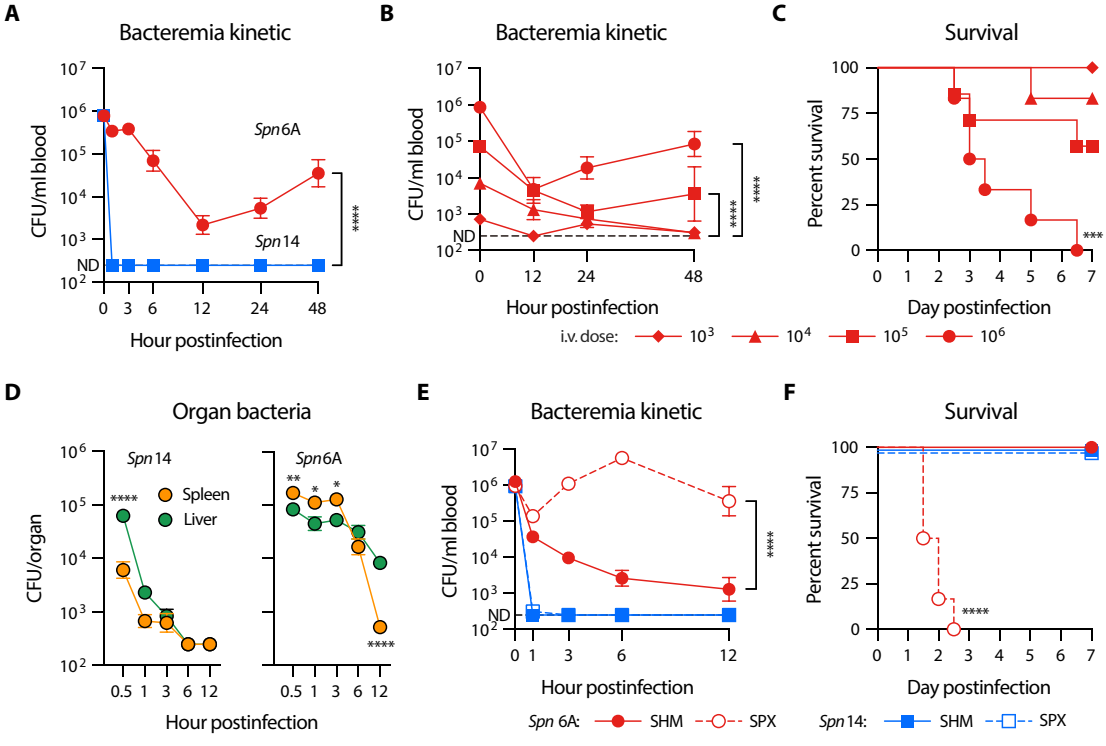

Fig. 1. Essential function of the spleen in clearing liver-resistant pneumococci. (**A**) Dramatic difference in the clearance kinetics of LV and HV pneumococci from the bloodstream of mice. Blood bacteria were monitored by retroorbital plexus bleeding and CFU counting at various time points post intravenous (i.v.) infection with 10^6 CFU LV serotype 14 (*Spn*14) or HV serotype 6A (*Spn*6A). $n = 6$ to 9. (**B**) Dose-dependent clearance of HV pneumococci. Blood bacteria were monitored in mice intravenously infected with 10^3, 10^4, 10^5, or 10^6 CFU *Spn*6A. $n = 5$ to 6. (**C**) Survival rate of mice post intravenous infection with various doses of *Spn*6A. (**D**) Differential distribution of LV and HV pneumococci in the liver and spleen. Bacterial loads were counted at various time points post intravenous infection with 10^6 CFU *Spn*14 or *Spn*6A. $n = 3$ to 6 at each time point. (**E**) Impact of splenic removal on the clearance of HV pneumococci from the bloodstream. Blood bacteria of SHM and SPX mice were monitored during the first 12 hours post intravenous infection with 10^6 CFU *Spn*14 or *Spn*6A. $n = 6$. (**F**) Survival rate of SHM and SPX mice post intravenous infection with 10^8 CFU *Spn*14 or 10^3 CFU *Spn*6A. $n = 6$. Dotted line indicates the detection limit [(A), (B), (D), and (E)]. Significance was compared by two-way analysis of variance (ANOVA) [(A), (B), (D), and (E)] and log-rank test [(C) and (F)]. $^*P < 0.05$, $^{**}P < 0.01$, $^{***}P < 0.001$, $^{****}P < 0.0001$.

mice infected with 10^5 (3500 CFU/ml) and 10^6 CFU (83,000 CFU/ml). This dose-dependent bacterial clearance indicated that this uncharacterized immunity is only able to clear relatively lower levels of blood-borne HV pneumococci. This conclusion is supported by a challenge dose-dependent survival of *Spn*6A-infected mice. All the mice in the group of 10^3 CFU survived the infection, whereas those receiving higher doses showed partial (10^4 and 10^5 CFU) or no (10^6 CFU) survival (Fig. 1C). This trial revealed a median lethal dose of 1.3×10^5 CFU for *Spn*6A in the intravenous infection route.

To determine how the liver-resistant pneumococci are cleared, we compared the levels of LV and HV pneumococci in the major organs at various time points post intravenous inoculation. As reported in our previous work (*17*), *Spn*14 bacteria were predominantly trapped in the liver at the onset of blood infection and became undetectable at 6 to 12 hours, but *Spn*6A pneumococci were more abundant in the spleen than liver in the first 3 hours and reduced to barely detectable level at 12 hours (Fig. 1D). Consistently, mice lacking KCs did not show obvious deficiency in clearing *Spn*6A in the first 12 hours of blood infection (fig. S1D). These results indicated that HV pneumococci are eliminated by a liver-independent immune mechanism in the spleen. To test this hypothesis, we compared bacteremia kinetics between asplenic and normal mice. In contrast to dramatic reduction in *Spn*6A bacteremia in sham-operated (SHM) mice in the first 12 hours of blood infection, splenectomized (SPX) mice showed apparent defect in controlling the HV bacteria, with higher bacteremia during this period (Fig. 1E). The importance of the spleen in clearing HV pneumococci was also evidenced by the hyper-susceptibility of SPX mice to *Spn*6A; all SPX mice died in 3 days post intravenous infection with an otherwise nonlethal dose (10^3 CFU) (Fig. 1F). Consistent with liver-based immunity against LV bacteria (*17*), SPX mice were full competent in clearing *Spn*14 (Fig. 1E) and withstood intravenous infection with a high dose (10^8 CFU) of *Spn*14 (Fig. 1F). These results demonstrated that the spleen is the major immune organ to eliminate the liver-resistant HV pneumococci in the early phase of blood infection.

RP macrophages are essential for splenic elimination of the liver-resistant pneumococci

To identify the splenic immune cells that are responsible for clearing HV pneumococcus, we first tested the splenic macrophages by selective depletion with clodronate liposomes (fig. S2) (*35*) because opposing roles of splenic macrophages have been reported in terms of their roles in antibacterial immunity (*25*, *27*, *32*). As compared with control mice, depleting both MZ and MP macrophages with a low-dose of clodronate liposomes (Low CL) did not yield apparent impact on the clearance of *Spn*6A in the first 12 hours post intravenous infection (Fig. 2A), suggesting that MZ and MP macrophages are dispensable for splenic clearance of HV pneumococci. In contrast, additional depletion of RP macrophages with a higher dose of clodronate liposomes (High CL) resulted in dramatic impairment in *Spn*6A clearance (Fig. 2A). Since the extent of immune dysfunction in high CL–treated mice was highly similar to what was observed in SPX mice (Fig. 1E), this result strongly suggested that RP macrophages are the major immune cells for clearing the liver-resistant pneumococci.

We verified the unique importance of RP macrophages in splenic clearance of HV pneumococci using *Spic*$^{-/-}$ mice (with a deficiency in RP macrophage development) (*36*) or *Nr1h3*$^{-/-}$ mice lacking both MZ and MP macrophages (fig. S2) (*37*). *Spic*$^{-/-}$ mice showed a similar extent of severe functional deficiency as high CL-treated and SPX mice in clearing HV pneumococci, with sustained bacteremia in the first 12 hours post intravenous inoculation of *Spn*6A, whereas *Nr1h3*$^{-/-}$ mice displayed a virtually normal pattern of bacterial clearance as wild-type (WT) control (Fig. 2B). Reduction of RP macrophages also led to uncontrolled bacterial replication in the spleen and liver (fig. S3A). In a similar fashion, all of *Spic*$^{-/-}$ mice succumbed to intravenous infection with nonlethal dose of *Spn*6A (10^3 CFU) in 2 days, but there was no mortality in *Nr1h3*$^{-/-}$ mice (Fig. 2C). These results demonstrated that RP macrophages are the major splenic macrophages for eliminating HV pneumococci in the "eclipse phase" of blood infection.

We further characterized pneumococcus-macrophage interaction by analyzing the spleen sections with immunofluorescence microscopy. Consistent with the dominant role of RP macrophages in bacterial clearance, the green fluorescent protein (GFP)–labeled *Spn*6A were predominantly colocalized with F4/80-labeled RP macrophages in the RP of WT mice (Fig. 2D, top). Relatively fewer bacteria were found in the MZ where CD169-labeled MP macrophages were located. Pneumococcal dominance in RP over MZ was diminished in *Spic*$^{-/-}$ mice (Fig. 2D, bottom) in terms of bacterial numbers per area of anatomical structure (Fig. 2E). After being normalized by the area size of each compartment in the spleen section (fig. S3B), approximately 90% bacteria were constrained in RP in WT mice, while the bacteria were uniformly distributed in the RP and MZ in *Spic*$^{-/-}$ mice (Fig. 2F). These microscopic observations provided additional evidence to support the unique antipneumococcal activity of RP macrophages in the spleen.

RP macrophages are capable of phagocytic killing of pneumococci

To understand how RP macrophages eradicate HV pneumococci, we carried out systemic analyses of the antibacterial function of splenic phagocytes. We first determined the roles of neutrophils and inflammatory monocytes (IMs) given the previous report that neutrophils are required to kill pneumococci captured by RP macrophages (*25*). Flow cytometry analysis showed dramatic increase in neutrophils and IMs in the first 6 hours of HV infection (Fig. 3A and fig. S4, A and B), which was effectively diminished by antibody depletion (fig. S4C). In contrast to dramatic impairment of RP macrophage–deficient mice in bacterial clearance, depleting neutrophils with 1A8 antibody did not yield obvious impact on bacteremia kinetics post intravenous inoculation (Fig. 3B). Likewise, *Ccr2*$^{-/-}$ mice with the deficiency in IM recruitment (*38*) did not exhibit notable defect in pneumococcal clearance (Fig. 3B). Unexpectedly, simultaneous depletion of both neutrophils and IMs using Gr1 antibody even enhanced pneumococcal clearance at the early time points (3 and 6 hours). Although Gr1-treated mice displayed functional deficit at the later stage (12 hours), the blood bacteria were still 15-fold lower than that in *Spic*$^{-/-}$ mice (Fig. 3B), as well as 150- and 35-fold lower bacterial burdens in the spleen and liver (fig. S4, D and E). The dominance of RP macrophages in bacterial capture was further supported by flow cytometry analysis of pneumococcal distribution among splenic phagocytes (fig. S4F). The total number of *Spn*6A-positive cells was threefold fewer in *Spic*$^{-/-}$ mice compared to the WT mice due to a dramatic reduction of bacterial binding to RP macrophages, which account for most *Spn*6A-associated splenocytes (Fig. 3, C and D). In contrast, depletion with Gr1 antibody even led to slightly higher bacterial capture despite loss of

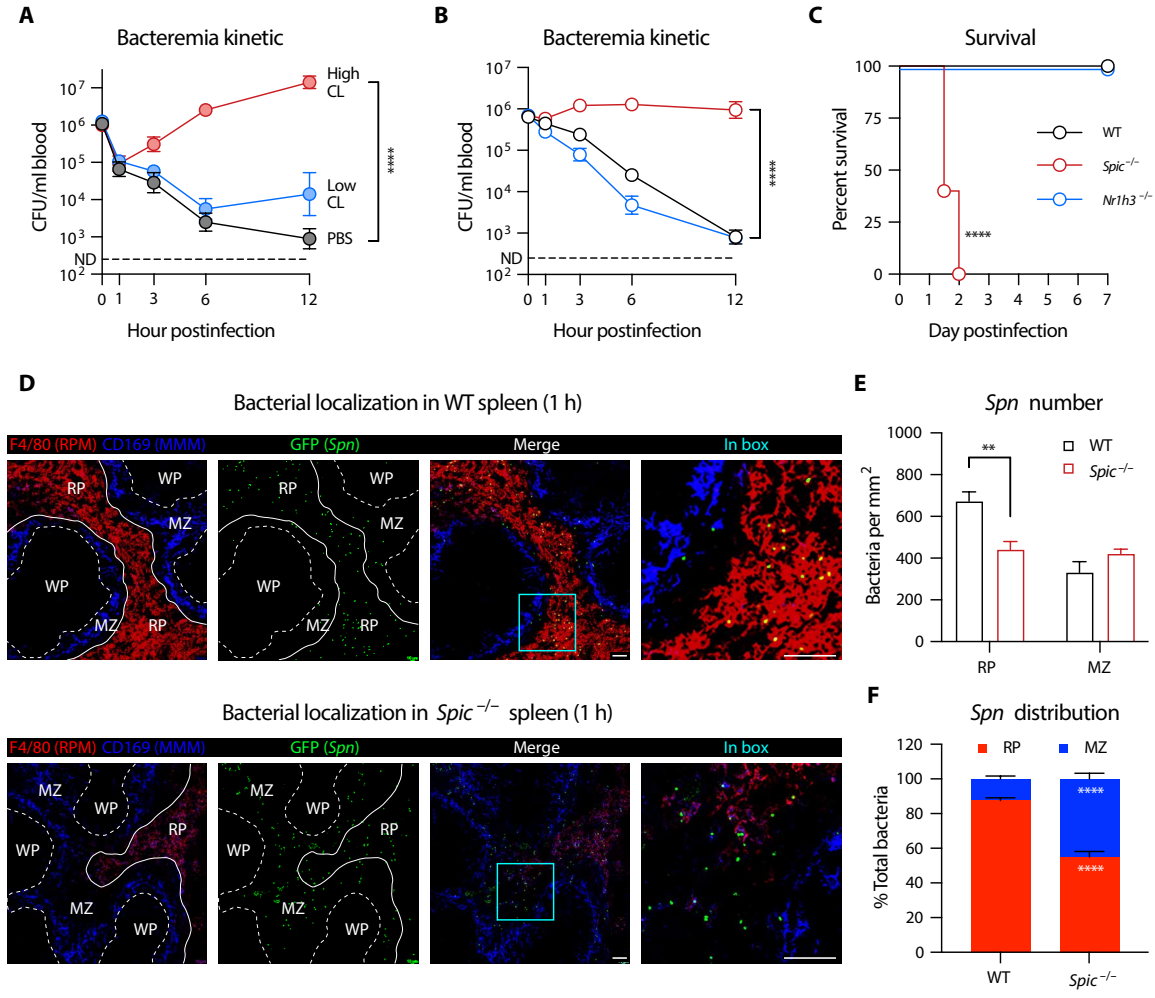

Fig. 2. The importance of RP macrophages in splenic control of HV pneumococci. (**A**) Impact of macrophage depletion on the clearance of HV pneumococci. Blood bacteria were monitored in mice that were pretreated with Low CL or High CL and intravenously infected with 10^6 CFU *Spn*6A. $n = 3$ to 6. (**B**) Essentiality of RP macrophages for the removal of HV pneumococci. Bacterial kinetics in the bloodstream were monitored in RP macrophage–deficient *Spic*$^{-/-}$ mice or *Nr1h3*$^{-/-}$ mice lacking both MZ and MP macrophages post intravenous infection with 10^6 CFU *Spn*6A. $n = 6$. (**C**) Survival of *Spic*$^{-/-}$ and *Nr1h3*$^{-/-}$ mice post intravenous infection with 10^3 CFU *Spn*6A. $n = 6$. (**D**) Representative immunofluorescent images to show bacterial trapping in splenic RP of WT and *Spic*$^{-/-}$ mice. Mice were intravenously infected with 10^7 CFU *Spn*6A-GFP (green) and splenic sections were prepared at 1 hpi. RP and MP macrophages were stained by AF647 anti-F4/80 (red) and AF594 anti-CD169 (blue), respectively. (**E** and **F**) Quantitative analysis of the imaging data in (D). Bacteria in 1 mm^2 per area of the RP and MZ were counted (E). Normalized bacteria distribution (F) was calculated by multiplying bacterial number per area by the total area of RP or MZ in the splenic section. $n = 5$ random fields of view (FOVs). Scale bar, 40 μm. Dotted line indicates the detection limit [(A) and (B)]. Significance was compared by two-way ANOVA [(A), (B), (E), and (F)] and log-rank test (C). $^{**}P < 0.01$, $^{****}P < 0.0001$.

*Spn*6A binding to neutrophils (Fig. 3, C and D). These results suggested that neutrophils and IMs play a minor role in splenic elimination of HV pneumococci at the early stage of blood infection.

To understand the process of bactericidal action of RP macrophages, we applied a two-photon synthetic aperture microscopy (2pSAM) system to visualize the in situ pathogen-macrophage interaction during blood infection. The recently developed 2pSAM enables long-term imaging of deep tissues at a millisecond scale while maintaining 1000-fold reduction in phototoxicity as compared to traditional two-photon microscopy (*39*). We first observed the behaviors of RP macrophages and neutrophils in response to pneumococci in the spleen of normal mice. In contrast to fast and unidirectional movement of HV encapsulated bacteria in the liver sinusoids (*17*, *18*), pneumococci were flowing in the splenic RP without clear direction (Fig. 4, A and B, and movie S1), which agrees with the open blood system in the RP. Likewise, bacterial capture by RP macrophages occurred in a much less dramatic manner as compared with the swift and firm bacterial capture by KCs in the liver sinusoids. Many bacteria initially touched the immune cells and then moved away in a stop-go cycle (fig. S5A). In line with the flow cytometry analysis, we observed an evident infiltration of neutrophils within 2 hours post infection (hpi) (fig. S5B and movie S1). The development of RP macrophages is impaired as indicated by a shrink of F4/80-positive area in *Spic*$^{-/-}$ spleen, in which the RP showed a significantly lower level of immobilized pneumococci; however, the gradual capture of *Spn*6A was competent in the spleens of neutrophil- and IM-depleted mice (Fig. 4, A and B, and movie S2). This real-time observation further

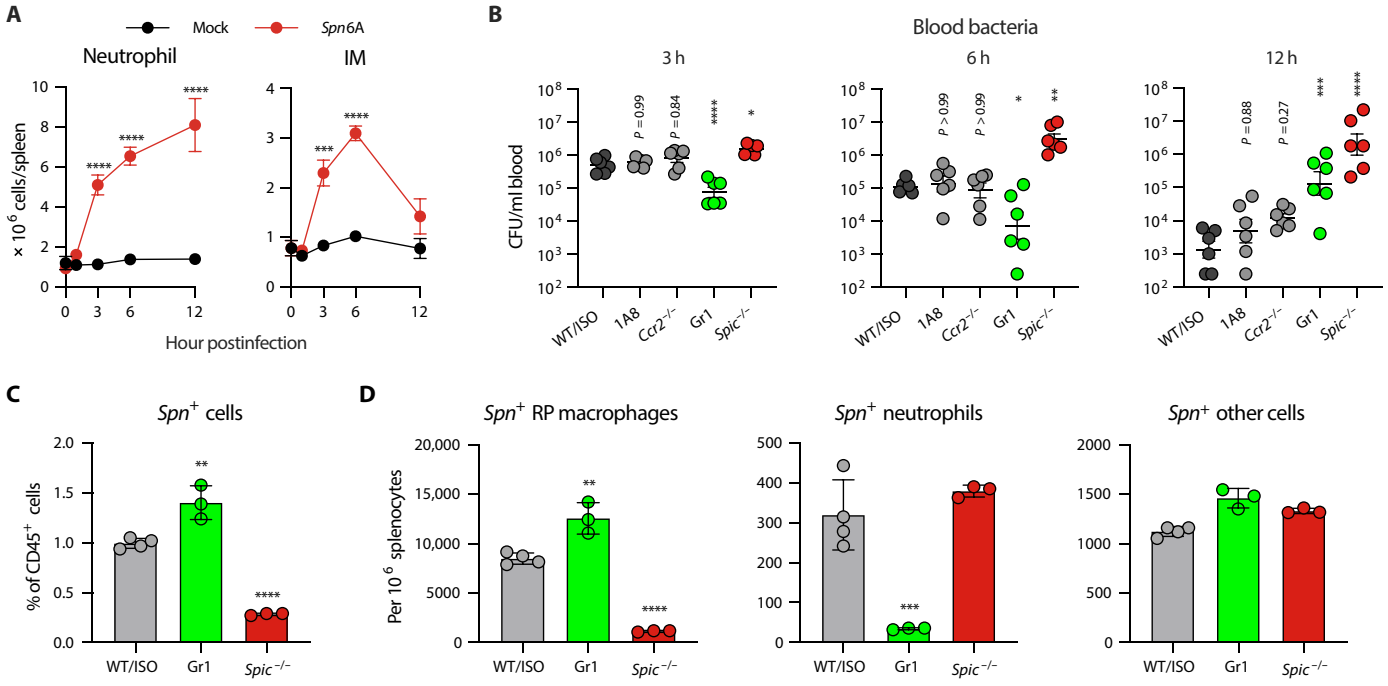

Fig. 3. Neutrophil-independent elimination of HV pneumococci by RP macrophages. (**A**) Infiltration of neutrophils and IMs in the spleen during pneumococcal infection. The kinetics of absolute numbers of neutrophils and IMs were assessed by flow cytometry post intravenous infection with 10^6 CFU of *Spn*6A. Mock-infected mice were intravenously injected with 100 μl of Ringer's solution. $n = 3$. (**B**) Impact of circulating phagocyte depletion on the clearance of HV pneumococci. Bacterial loads in the blood were counted at 3, 6, and 12 hpi with 10^6 CFU of *Spn*6A and compared among phagocyte-deficient mice. 1A8 or Gr1 antibodies depleted neutrophils or both neutrophils and IMs, respectively; *Ccr2*$^{-/-}$ mice were deficient in IM infiltration; *Spic*$^{-/-}$ mice lacked RP macrophage; ISO, isotype control. $n = 6$. (**C**) Ratio of pneumococcus-associated cells in splenocytes (CD45-positive cells) as detected by flow cytometry. Splenocytes were isolated from WT or isotype control, Gr1-treated, and *Spic*$^{-/-}$ mice at 30 min post intravenous infection with 10^7 CFU of GFP-expressing *Spn*6A. $n = 3$. (**D**) Quantification of pneumococcus-associated splenic phagocytes based on flow cytometry as in (C). Numbers of *Spn*-positive RP macrophages, neutrophils, and other CD11b$^+$ cells were calculated among every 10^6 of splenocytes. Detailed gating strategy was shown in fig. S4F. $n = 3$. Significance was compared by two-way (A) or one-way [(B) to (D)] ANOVA test. *$P < 0.05$, **$P < 0.01$, ***$P < 0.001$, ****$P < 0.0001$.

demonstrated the pivotal role of RP macrophages in eliminating the liver-resistant bacteria.

Next, we followed the destiny of the bacteria once being captured by RP macrophages. As previously reported (*25*), neutrophils were abundantly present in the RP and occasionally plucked the pneumococci from RP macrophage surface (Fig. 4C, top, and movie S3A). However, the vast majority of RP macrophages engulfed the immobilized pneumococci at the site far away from migrating neutrophils. The GFP signals were finally immersed in F4/80-positive cells, indicating intracellular digestion of the bacteria by RP macrophages (Fig. 4C, bottom, and movie S3B). Phagosome maturation after fusion with lysosome is the major way for intracellular killing of ingested bacteria, which is accompanied with acidification and oxidation in phago-lysosome (*40*). We thus tested whether the disappeared pneumococci were killed in the phago-lysosome of RP macrophages by using the indicative dye pHrodo Red (*41*). As expected, the pneumococcus-loaded probes were activated as early as 30 min post inoculation in both normal and Gr1-treated mice (Fig. 4D and fig. S5C). Notably, more pneumococci were embedded in the phago-lysosome of RP macrophages when neutrophils and IMs were depleted (66% inside) compared to the control (45% inside) (Fig. 4E), which was consistent with the accelerated bacterial clearance from the blood (3 and 6 hours; Fig. 3B). However, only 18% pneumococci were internalized when RP macrophages were defective (Fig. 4E). Consistent with the marginal impact of neutrophil depletion on splenic clearance of HV pneumococci, these imaging data demonstrated that RP macrophages are capable of phagocytic killing of capture pneumococci without the assistance of neutrophils.

RP macrophages use nAbs to clear the liver-resistant pneumococci

Our recent work has revealed that the liver KCs capture LV pneumococci by recognizing bacterial capsules through specific receptors (*17*). We thus reasoned that RP macrophages might use a similar strategy to capture HV pneumococci. To test this hypothesis, we conducted affinity screening by incubating beads coated with CPSs of HV pneumococcal serotypes with enriched membrane proteins of murine RP macrophages. However, our repeated trails did not consistently identify any RP macrophage membrane proteins potentially interacting with the HV capsules. This result implied that RP macrophages use an indirect manner to capture HV pneumococci, i.e., with the help of opsonins like antibody and complement proteins.

Given the fact that HV serotypes are highly proliferative in the blood of mice with genetic deficiency in nAb production (*42*, *43*), we tested whether nAbs are involved in RP macrophage–mediated pneumococcal clearance using B cell-deficient (μ*MT*) mice, which lack mature B cells and antibodies (*44*). μ*MT* mice showed severely compromised clearance of *Spn*6A, with stably sustained bacteremia in the first 6 hpi (Fig. 5A), although the functional

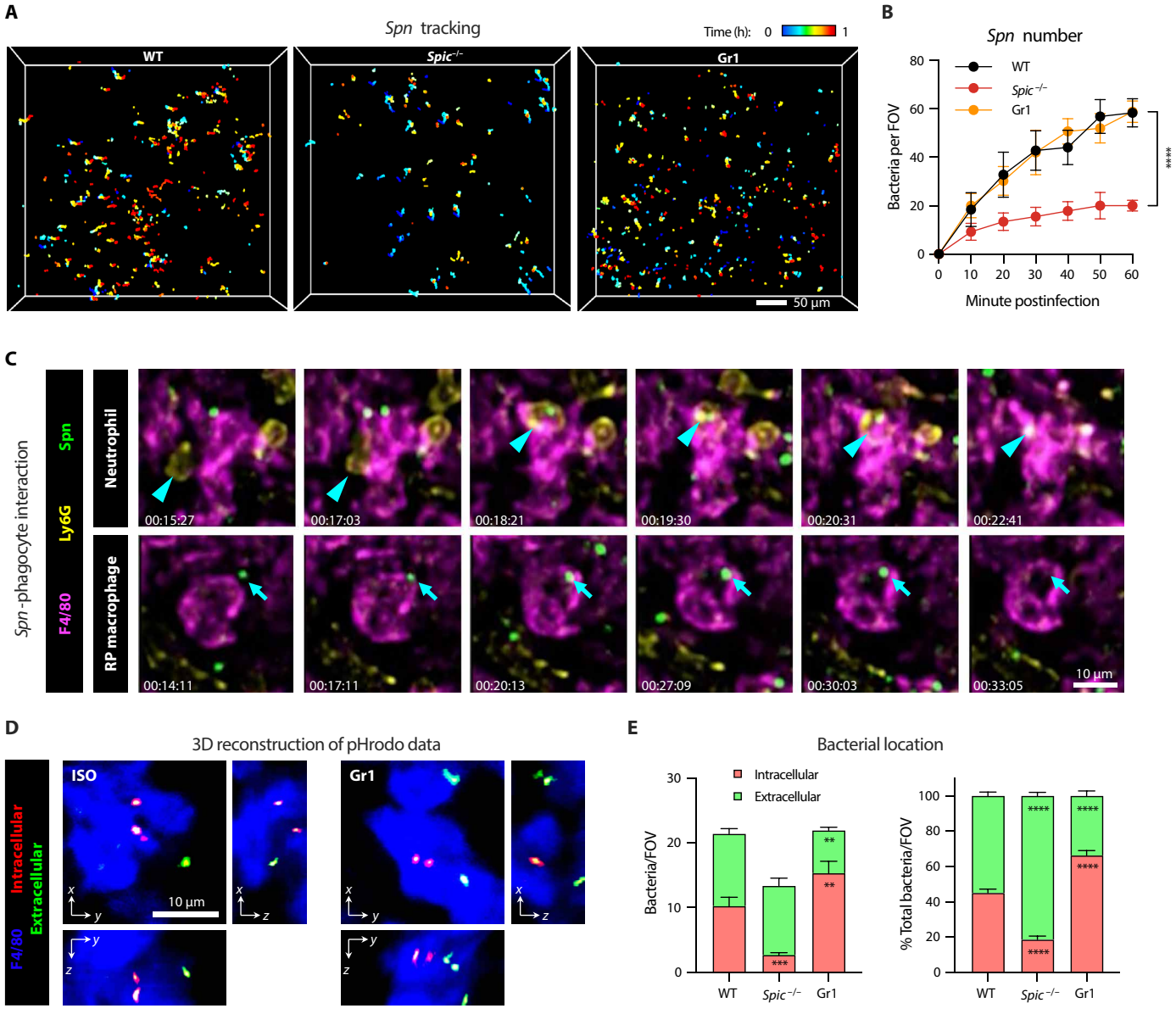

Fig. 4. Illustration of RP macrophage–executed pneumococcal clearance by IVM. (**A**) 2pSAM illustration of pneumococcal tracking in the spleens of WT, *Spic*$^{-/-}$, and Gr1 mice post intravenous infection with 5×10^6 CFU of *Spn*6A-GFP (movie S2). Pneumococci trapped in the field for at least 1 min were recorded during the first hour postinfection. Scale bar, 50 µm. (**B**) Number of trapped pneumococci in the field during the first hour as monitored by 2pSAM in (A). $n = 10$ to 15 random FOVs. (**C**) Representative consecutive 2pSAM imaging to show the neutrophil-dependent elimination (top, movie S3A) and direct elimination by single RP macrophage (bottom, movie S3B) of *Spn*6A in the spleen of WT mice. Arrows and arrowheads indicate *Spn* cells and neutrophils, respectively. Scale bar, 10 µm. (**D**) Representative three-dimensional reconstruction of 2pSAM images to illustrate the uptake of pneumococci by RP macrophages. Internalization of *Spn*6A cells were labeled with pHrodo Red and intravenously injected into ISO and Gr1-treated mice. Internalization of bacteria was indicated by the activation of pHrodo Red under acid environment, i.e., in the phagolysosomes of RP macrophages. Images were obtained at 1 hpi. Scale bar, 10 µm. (**E**) Quantification of pneumococcal uptake by RP macrophages. The number (left) and ratio (right) of intra- and extracellular pneumococci in the spleens of WT, *Spic*$^{-/-}$, and Gr1-treated mice were analyzed at 1 hpi. $n = 10$ random FOVs. Significance was compared by two-way ANOVA [(B) and (E)] test. $^{**}P < 0.01$, $^{***}P < 0.001$, $^{****}P < 0.0001$.

deficit in µ*MT* mice was less pronounced than in asplenic mice (Fig. 1E) and *Spic*$^{-/-}$ mice (Fig. 2B) during 6 to 12 hpi. We next assessed whether purified serum antibodies enhance pneumococcal clearance in µ*MT* mice. Enzyme-linked immunosorbent assay (ELISA) test revealed that normal murine serum contains substantial level of immunoglobulin M (IgM) antibodies and, to a less extent, of IgG antibodies targeting *Spn*6A pneumococci (fig. S6A). Pre-opsonization with purified natural IgM (nIgM) or nIgG restored the capacity of µ*MT* mice to clear *Spn*6A in a dose-dependent manner (Fig. 5B). Moreover, the nIgM antibodies were more efficient than nIgG in promoting pneumococcal clearance especially in the early time points, e.g., 3 and 6 hpi (Fig. 5B). These results suggested that RP macrophages use serum antibodies to clear the liver-resistant pneumococci.

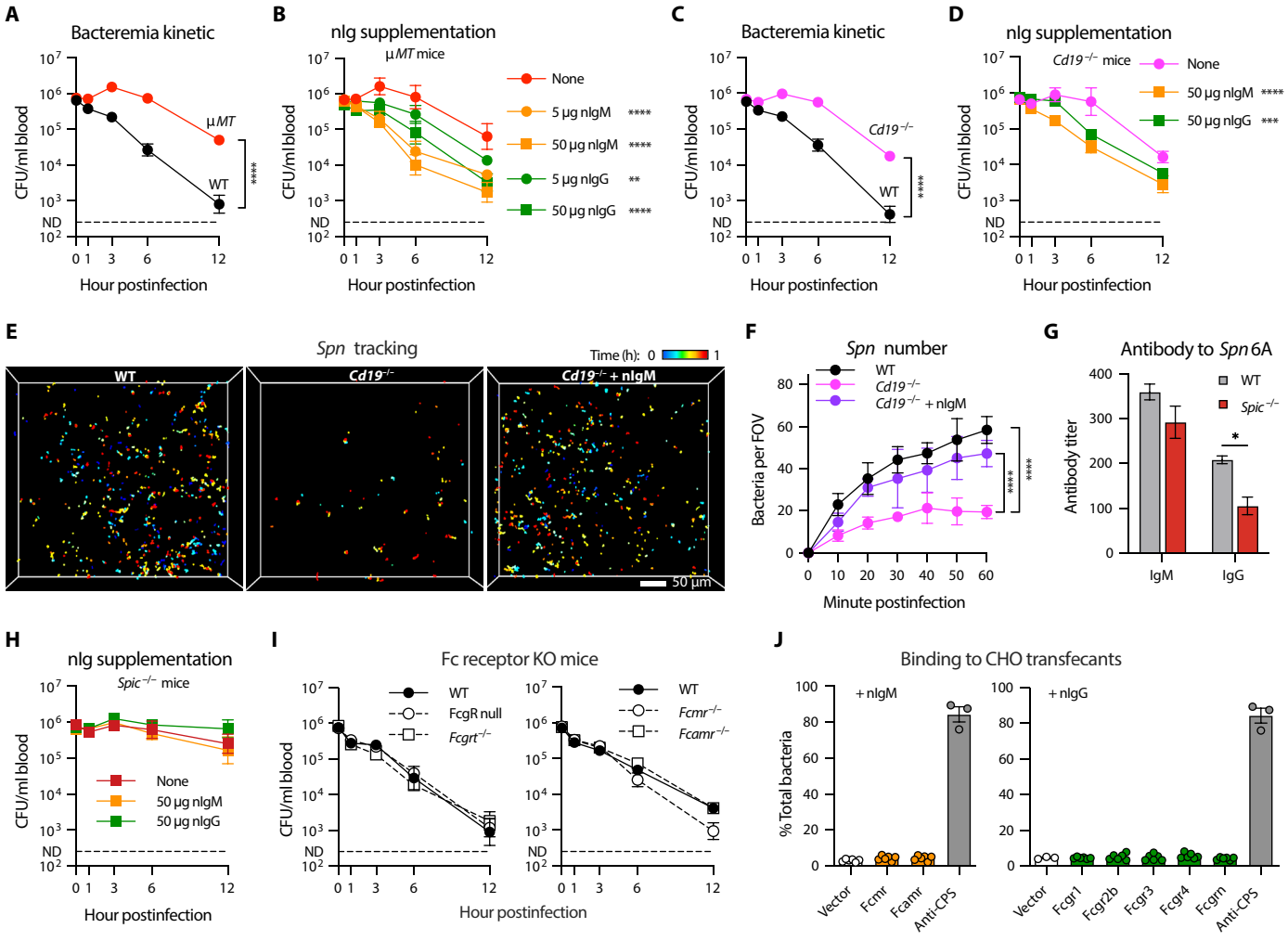

Fig. 5. The essential role of nAbs in splenic clearance of HV pneumococci. (**A**) Early-phase bacteremia kinetic in WT and antibody-null (*μMT*) mice post intravenous infection with 10^6 CFU of *Spn*6A. $n = 6$. (**B**) Dose-dependent promotion of *Spn*6A clearance by purified nIgM and nIgG in *μMT* mice. $n = 4$ to 6. (**C**) Early-phase bacteremia kinetic in WT and B1 cell–deficient ($Cd19^{-/-}$) mice postinfection as in (A). $n = 6$. (**D**) Promotion of *Spn*6A clearance by nIgM and nIgG in $Cd19^{-/-}$ mice. $n = 3$. (**E**) 2pSAM illustration of pneumococcal tracking in the spleens of WT and $Cd19^{-/-}$ mice postinfection with 5×10^6 CFU of native *Spn*6A-GFP or pre-opsonized with 50 μg of nIgM ($Cd19^{-/-}$ + nIgM, movie S4). Scale bar, 50 μm. (**F**) Number of trapped pneumococci in the field during the first hour as monitored by 2pSAM in (E). $n = 10$ to 15 random FOVs. (**G**) Titers of anti-*Spn*6A nIgM and nIgG in the serum of WT and $Spic^{-/-}$ mice. $n = 3$. (**H**) Early-phase bacteremia kinetic in $Spic^{-/-}$ mice postinfection with 10^6 CFU of nIgM- or nIgG-opsonized *Spn*6A. $n = 3$ to 6. (**I**) Dispensable role of well-known Fc receptors for HV pneumococcal clearance. Bacteremia kinetics were monitored in all known Fc gamma receptors-deficient (FcgR null and $Fcgrt^{-/-}$) and putative Fc miu receptor–deficient ($Fcmr^{-/-}$ and $Fcamr^{-/-}$) mice postinfection as in (A). $n = 3$. (**J**) In vitro binding of T15 IgM- or IgG3-coated HV pneumococci to CHO transfectants. *Spn*6A was incubated with the CHO cells [multiplicity of infection (MOI) 1] for 1 hour in the presence of T15 antibodies (50 μg/ml). Anti-CPS IgG1 was used as positive control. $n = 3$. Significance was compared by two-way ANOVA test [(A) to (D) and (F), and (G)]. $^{***}P < 0.001$, $^{****}P < 0.0001$.

To distinguish the role of nAbs produced by B1 cells from antibodies generated by antigen-stimulated B2 cells, we assessed pneumococcal clearance in B1-deficient $Cd19^{-/-}$ mice, which lack nAbs (*45*). The $Cd19^{-/-}$ mice showed similar functional deficiencies in producing antipneumococcal antibodies (fig. S6A) and clearing *Spn*6A from the bloodstream as *μMT* mice (Fig. 5C). The bacterial clearance was substantially recovered when the *Spn*6A pneumococci were precoated with purified nIgM and, to a less extent, purified nIgG (Fig. 5D). The functional impairment of bacterial clearance was further confirmed by intravital 2pSAM. The number of trapped *Spn*6A-GFP in the spleens of $Cd19^{-/-}$ mice was significantly fewer than that in WT controls within 1 hour of observation (Fig. 5, E and F, and movie S4A). This immune defect was substantially reversed by opsonization of the *Spn*6A with 50 μg of purified nIgM (Fig. 5, E and F, and movie S4B). We finally investigated the necessity of RP macrophages for nAb-mediated pneumococcal clearance using $Spic^{-/-}$ mice, which produce normal level of nIgM but less IgG targeting *Spn*6A cells (Fig. 5G). Nevertheless, precoating with high doses of purified nIgM or nIgG did not improve bacterial clearance in $Spic^{-/-}$ mice (Fig. 5H). These results showed that B1 cell–derived nAbs are essential for RP macrophage–mediated clearance of HV pneumococci in the spleen.

We next investigated how nAbs enable RP macrophages to clear circulating pneumococci. Current understanding of the antibody

effector mechanisms for bacterial elimination include direct recognition by corresponding Fc receptors (*46*) and activation of the complement system via classical pathway (*47*). Our recent work has revealed that vaccine-elicited anti-capsule antibodies enable liver KCs to capture circulating pneumococci through multiple Fc receptors (*48*). Thus, we tested whether RP macrophages use a similar mechanism to capture HV pneumococci by investigating the roles of Fc receptors. Our proteomic analysis detected the expression of FcγRIIB, FcγRIII, FcγRIV, and FcRn on murine RP macrophages, four of the five known FcγRs in mice (fig. S6B). Contrary to our expectation, the FcγR null mice with complete knockout (KO) of FcγRI/IIb/III/IV (*49*) as well as FcRn KO (*Fcgrt*$^{-/-}$) mice displayed comparable levels of pneumococcal clearance as WT counterparts (Fig. 5I, left). Similar results were observed using mice lacking FcμR or FcαμR (Fig. 5I, right), the two known IgM receptors (*50*, *51*). To address the potential functional redundancy among these Fc receptors, we conducted a gain-of-function approach by overexpressing the individual receptor in Chinese hamster ovary (CHO) cells and assessing pneumococcal binding to the transfectants in the presence of T15 monoclonal antibodies. However, stable expression of the two FcμRs or five FcγRs did not lead to a notable increase in adhesion (less than 5%) of T15 IgM- or IgG3-opsonized *Spn*6A to CHO cells compared to the pronounced enhancement (85% binding) by anti-capsule antibodies (Fig. 5J). Collectively, the in vivo and in vitro data suggested that anti-phosphocholine (PC) nAbs contribute to HV pneumococcal clearance through activating the complement system instead of engaging antibody receptors as the capsule-targeting antibodies (*48*).

Protective nAbs target pneumococcal cell wall PC

To ascertain how nAbs enable RP macrophages to clear HV pneumococci, we characterized pneumococcal antigens that are recognized by the antibodies. Given our finding that the splenic antibacterial immunity is effective against multiple HV serotypes of *S. pneumoniae* (see below), we reasoned that protective nAbs must target a conserved antigen beyond the capsule structure. Consistently, administration of purified serotype 6A CPS before intravenous inoculation of *Spn*6A showed little impact on the bacterial clearance during the eclipse phase (fig. S7A). These results suggested that RP macrophages recognize non-capsular ligands on HV pneumococci. The cell wall PC or C polysaccharide is the only known pneumococcal antigen that is recognized by protective nAbs (*42*, *52*). We verified the existence of anti-PC antibodies in normal mouse serum by ELISA, in which the IgM and IgG titers were significantly lower using PC-free *Spn*6A whole cells as antigen compared to intact pneumococci (Fig. 6A). The assessment also revealed substantial amounts of anti-PC IgM and IgG in normal mouse serum (Fig. 6A) and purified nAbs (fig. S7B). We extended this investigation to the adult human serum and observed a consistent pattern. Both IgM and IgG titers were markedly reduced against PC-free *Spn*6A compared to responses elicited by intact bacteria, which corroborated the existence of substantial levels of PC-reactive IgM and IgG in human serum (Fig. 6B).

To test whether RP macrophages depend on anti-PC antibodies to eliminate HV pneumococci, we performed a passive protection experiment in *Cd19*$^{-/-}$ mice with purified nAbs that were preabsorbed with PC-coated resin. Pre-opsonization with PC-absorbed nIgM showed weakened activity in promoting *Spn*6A clearance in *Cd19*$^{-/-}$ mice as compared with the native nIgM, particularly at 3 and 6 hpi (Fig. 6C). To verify the specific role of anti-PC antibodies, we generated the IgM and IgG3 forms of anti-PC monoclonal antibodies of the T15 idiotype (*53*), which have been known to protect mice against pneumococcal disease (*54*, *55*). Opsonization with both T15 IgM and IgG3 potently rescued pneumococcal clearance in *Cd19*$^{-/-}$ mice even at a low dose, e.g., 5 μg (Fig. 6D). We next monitored the in vivo behavior of pneumococci in the presence of T15 antibodies using 2pSAM. The T15 IgM was chosen because of its higher levels in antigen binding (fig. S7C) and in promoting pneumococcal clearance (Fig. 6D). As expected, the long-term observation revealed sporadic *Spn*6A-GFP that is trapped in the spleen of *Cd19*$^{-/-}$ mice; this functional deficiency was fully recovered by pre-opsonization with T15 IgM (Fig. 6, E and F, and movie S5). These functional investigation and real time illustration demonstrated that RP macrophages use anti-PC nAbs to clear the liver-resistant pneumococci. The C-reactive protein (CRP) has long been known as an important pentraxin that reacts with the PC moiety of pneumococcal C polysaccharide (*56*); however, the *Crp*$^{-/-}$ mice were still able to clear the HV *Spn*6A in the first 12 hpi (fig. S7D). This result indicated an essential role of nAbs in the splenic control of the liver-resistant pneumococci.

Since the importance of the anti-PC nAbs in clearing HV pneumococci, we next determined whether supplementation of anti-PC antibodies in normal mice could improve the bacterial clearance and rescue fatal infection. Pre-opsonization with monoclonal T15 IgM led to accelerated *Spn*6A clearance from the blood of WT mice in a dose-dependent manner. Whereas pretreated with a low dose (1 μg) of T15 IgM resulted in mildly enhanced bacterial clearance in the first 12 hpi, the blood bacteria were rapidly removed when using a high dose (50 μg) of T15 IgM as early as in 1 hpi (Fig. 6G). The blood bacteria were maintained at low levels in 2 days in the mice infected with extensively opsonized *Spn*6A compared to the regrowth of bacteria at later stage without or with the low-dose antibody treatment (Fig. 6H). Accordingly, the high-dose antibody treatment led to complete elimination of *Spn*6A in half of the mice that were rescued from the lethal infection (Fig. 6I). These data suggested the anti-PC antibodies as a potential therapeutic choice to treat blood infection caused by HV pneumococci.

Complement C3 is necessary for the splenic clearance of HV pneumococci

In the context of the abovementioned data, we investigated the potential involvement of the complement system in activating the anti-HV pneumococcal immunity of RP macrophages using *C3*$^{-/-}$ mice (*57*), which lack the core complement protein C3. Similar to the RP macrophage– and antibody-deficient mice, the *C3*$^{-/-}$ animals showed significant impairment in clearing *Spn*6A pneumococci from the circulation. The *C3*$^{-/-}$ mice showed remarkably higher levels of bacteremia at all of the tested time points in the first 12 hpi with 10^6 CFU of *Spn*6A as compared with WT (Fig. 7A). Accordingly, the blood bacterial burden at 24 hpi in *C3*$^{-/-}$ mice was 1700-fold higher than the WT (Fig. 7B), leading to the 100% mortality in 36 hpi (Fig. 7C, left). Notably, all of the tested *C3*$^{-/-}$ mice succumbed to the infection with 10^3 CFU of *Spn*6A, an otherwise nonlethal dose (Fig. 7C, right). In addition, the cultured primary RP macrophages showed a substantial level of binding to *Spn*6A bacteria that were pre-opsoinzed with normal serum, while the bacterial binding was significantly decreased when using *C3*$^{-/-}$ serum for opsonization (Fig. 7D). These results strongly suggested that the

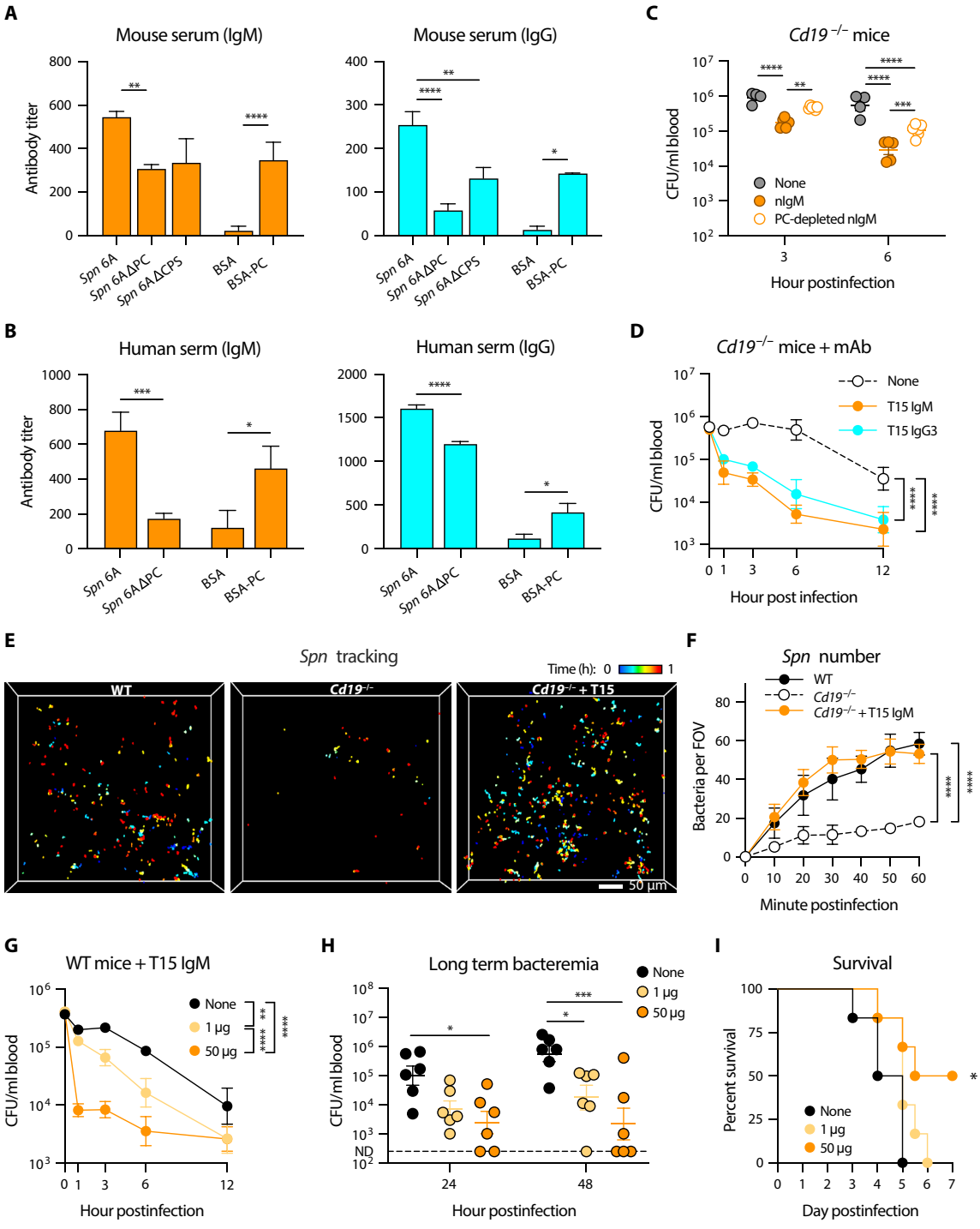

Fig. 6. Pneumococcal cell wall PC as a target antigen of nAbs. (**A** and **B**) Detection of anti-PC nAbs in normal murine (A) and human (B) serum. Titers of IgM (left) and IgG (right) were measured by ELISA using *Spn*6A whole cells, *Spn*6A lacking PC or CPS, and BSA-conjugated PC as antigens. $n = 3$. (**C**) Importance of anti-PC nAbs for HV pneumococcal clearance. Blood bacterial loads were counted in *Cd19*$^{-/-}$ mice postinfection with 10^6 CFU of *Spn*6A that was untreated, pre-opsonized with 50 μg of native nIgM or PC resin–absorbed nIgM. $n = 4$ to 6. (**D**) Promotion of HV pneumococcal clearance by monoclonal anti-PC IgM and IgG3. Bacteremia kinetics were monitored in *Cd19*$^{-/-}$ mice postinfection with 10^6 CFU of *Spn*6A pre-opsonized with 5 μg monoclonal T15 anti-PC IgM and IgG3. $n = 6$. (**E**) 2pSAM illustration of pneumococcal tracking in the spleens of WT and *Cd19*$^{-/-}$ mice postinfection with 5×10^6 CFU of native *Spn*6A-GFP or pre-opsonized with 25 μg T15 IgM (*Cd19*$^{-/-}$ + T15, movie S5). Scale bar, 50 μm. (**F**) Number of trapped pneumococci in the field during the first hour as monitored by 2pSAM in (E). $n = 10$ to 15 random FOVs. (**G** to **I**) Dose-dependent immune protection by anti-PC antibodies against pneumococcal infection. Bacteremia kinetics in the first 12 hours (G), at 24 and 48 hours (H), and survival (I) were assessed in WT mice postinfection with 10^6 CFU of *Spn*6A that was untreated or pre-opsonized with low (1 μg) or high (50 μg) dose of T15 IgM. $n = 6$. Significance was compared by one-way [(A) and (B)] or two-way [(C) and (D) and (F) to (H)] ANOVA and log-rank test (I). $^*P < 0.05$, $^{**}P < 0.01$, $^{***}P < 0.001$, $^{****}P < 0.0001$.

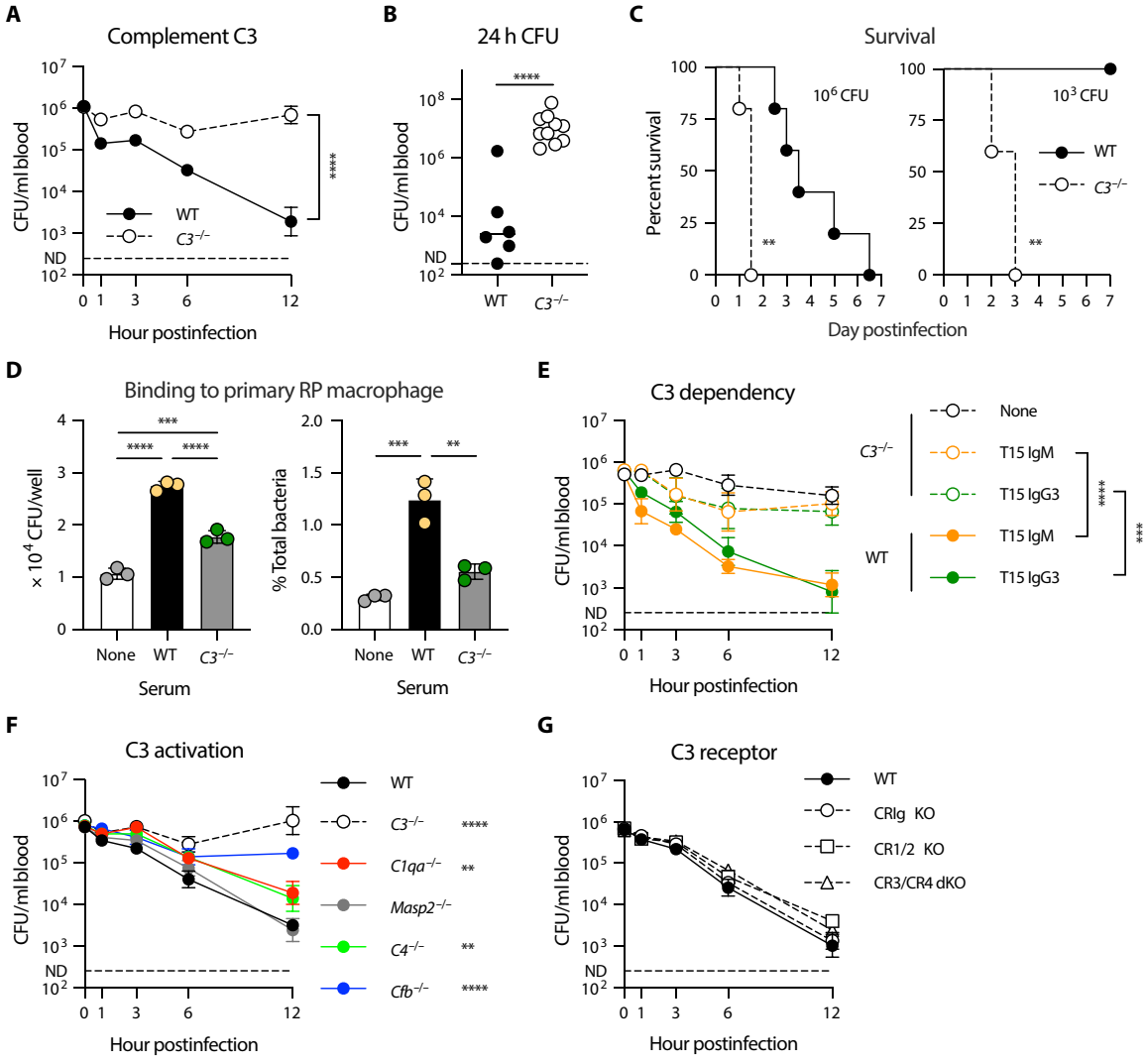

Fig. 7. The requirement of complement C3 for the clearance of HV pneumococci in the spleen. (**A** to **C**) Pivotal role of complement C3 for the innate immune defense against HV pneumococci. Blood bacterial loads were counted in the first 12 hours (A) and at 24 hours (B) postinfection with 10^6 CFU of *Spn*6A in WT and $C3^{-/-}$ mice. $n = 6$ to 10. Survival (C) were monitored postinfection with high dose (10^6 CFU, left) or low dose (10^3 CFU, right) of *Spn*6A. $n = 5$. (**D**) In vitro binding of HV pneumococci to primary RP macrophages. *Spn*6A was pre-opsonized by WT or $C3^{-/-}$ serum and incubated with the primary RP macrophages for 30 min at MOI of 1. $n = 3$. (**E**) Requirement of complement C3 for anti-PC antibody-mediated clearance of HV pneumococci. Blood bacterial loads were counted in the first 12 hours in WT and $C3^{-/-}$ mice postinfection with 10^6 CFU of *Spn*6A that pre-opsonized by 5 μg of T15 IgM or IgG3. $n = 5$. (**F**) Role of complement activation pathways in the immune clearance of HV pneumococci. Blood bacterial loads were compared in the first 12 hours in each mouse line postinfection with 10^6 CFU of *Spn*6A. $n = 3$ to 6. (**G**) Dispensable role of well-known complement receptors in the immune clearance of HV pneumococci. Blood bacterial loads in complement receptor–deficient mice were assessed as in (F). $n = 3$ to 6. Significance was compared by two-way [(A), (E), and (F)] or one-way ANOVA (D), Student's *t* (B), or log-rank (C) test. $^{**}P < 0.01$, $^{***}P < 0.001$, $^{****}P < 0.0001$.

complement-mediated innate immunity is involved in clearing the HV pneumococci in the early phase of septic infection.

To test the direct contribution of complement system on the antipneumococcal function of nAbs, we evaluated the bacterial clearance in $C3^{-/-}$ mice postinfection with T15 IgM- or IgG3-coated *Spn*6A. Although the anti-PC monoclonal antibodies promoted pneumococcal clearance from the bloodstream at 3 and 6 hpi, the bacteremia levels were still 10- to 20-fold higher in $C3^{-/-}$ mice than in WT controls. Notably, the $C3^{-/-}$ mice sustained a prominent bacterial burden in the blood during the first 12 hpi despite the presence of T15 antibodies compared with gradual clearance in WT mice (Fig. 7E). This in vivo assay demonstrated a pivotal role of the complement system in nAb-driven innate defense against HV pneumococci.

We next determined how nAb and the complement system work together to enhance the clearance of HV *S. pneumoniae* by RP macrophages. NAbs are known to activate the C3 protein via the classical activation pathway, with the help of complement proteins C1 and C4 (*47*). We thus tested the contribution of C1 and C4 to pneumococcal clearance using $C1qa^{-/-}$ and $C4^{-/-}$ mice (*58*). To our surprise, both the mouse lines showed marginal defect in eliminating *Spn*6A in the first 12 hours. Unexpectedly, the $Cfb^{-/-}$ mice lacking the alternative pathway activator protease factor B showed the most severe impairment in bacterial clearance (Fig. 7F), although there is no known

functional linkage between antibody and factor B in C3 activation. C3 is known to promote bacterial phagocytosis by binding to complement receptors on phagocytes (*59*). The previous study has shown that RP macrophages express both complement receptor 3 (CR3) and 4 (CR4) (*36*). However, simultaneous knock out of CR3 and CR4 did not result in apparent impact on the *Spn*6A clearance during the first 12 hpi (Fig. 7G). Together, these data have revealed an essential role of C3 in mediating nAb-driven bacterial clearance by RP macrophages in the spleen, but the precise mechanism of the antibody-complement functional linkage awaits further investigation.

The splenic antibacterial immunity operates across pneumococcal serotypes

Because PC is a conserved surface moiety and surface PC levels are relatively stable in *S. pneumoniae* strains (Fig. 8A) (*60*), we tested whether anti-PC nAb-mediated splenic immunity operates across capsular serotypes by assessing the bacteremia kinetics of HV serotypes 2, 3, 4 and 8. All the four serotypes were gradually cleared from the bloodstream in the early phase of infection, although the clearance rates varied among the serotypes (fig. S8A). However, the clearance immunity was completely lost by surgical removal of the spleen. As seen with *Spn*6A (Fig. 1E), asplenic mice showed notable increase in bacteremia level at various time points in the first 12 hours postinfection with serotypes 2, 3, 4, and 8 (Fig. 8B). In contrast, LV serotypes 19F and 23F bacteria were rapidly eliminated in both the asplenic mice and sham surgery controls in the first hour post inoculation and remained undetectable ever since (fig. S8, B and C). This information has revealed that the spleen is able to eliminate multiple liver-resistant pneumococcal serotypes.

We further verified the cellular and molecular mechanisms of the broad antibacterial immunity in the spleen using strain TIGR4 (serotype 4). Consistent with the data obtained with *Spn*6A (Fig. 2B), RP macrophage–deficient mice displayed persistent bacteremia in the first 12 hpi (Fig. 8C). Moreover, the antibody-deficient *Cd19*$^{-/-}$ mice exhibited remarkable deficiency in clearing TIGR4, particularly at the early time points, which could be reversed by pre-opsonizing the bacteria with the T15 antibody (Fig. 8D). In a similar manner, inoculation of TIGR4 pneumococci in the mice lacking complement C3 led to uncontrolled bacterial growth in the bloodstream at the early stage (Fig. 8E). These findings were verified with serotype-2 strain D39 (fig. S8, D to F). These data allowed us to conclude that RP macrophages, in concert with anti-PC nAbs and complement C3, are pivotal for splenic removal of various liver-resistant pneumococci.

Patients with chronic liver diseases are at higher risk in developing bacterial sepsis (*61*, *62*). We thus tested whether the spleen clears LV pneumococci in case the liver-based immunity is compromised using the LV serotype-14 pneumococci (*Spn*14). In line with the importance of liver-resident macrophages in eliminating LV pneumococci

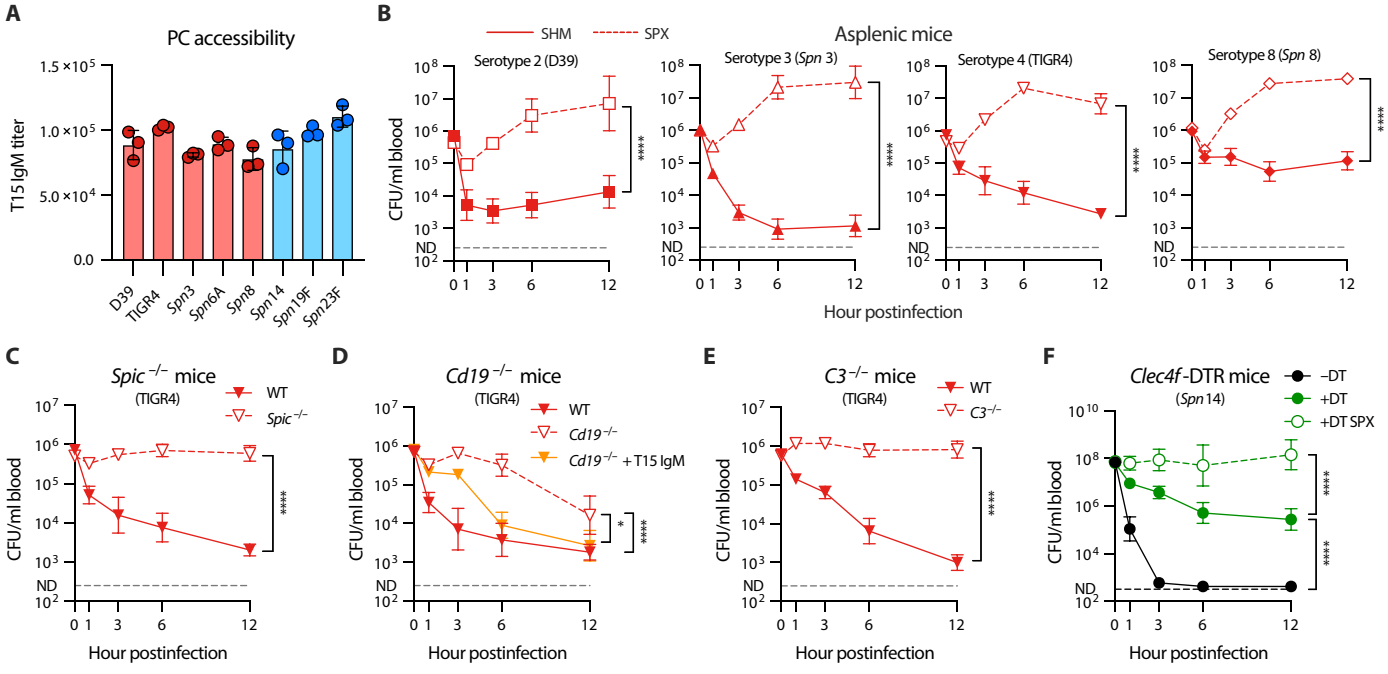

Fig. 8. Serotype-independent broad operation of splenic RP macrophage–mediated immunity against HV pneumococci. (**A**) Surface PC amounts in various pneumococcal strains. The PC accessibilities were reflected by the relative T15 IgM titers against WT strain D39 and TIGR4, as well as the isogenic capsule-switched strains in TH870 (*Spn*6A) background. (**B**) Importance of spleen for the blood clearance of multiple HV pneumococci. Blood bacterial loads in SPX mice were counted in the first 12 hours postinfection with 10^6 CFU of serotype 2 (D39), serotype 4 (TIGR4), and isogenic serotype 3 and 8 strains (*Spn*3 and *Spn*8), as compared with the SHM controls. $n = 3$. (**C**) Essential role of RP macrophages for the blood clearance of HV TIGR4. Blood bacterial loads in *Spic*$^{-/-}$ mice were counted in the first 12 hours postinfection with 10^6 CFU of TIGR4 and compared with the WT controls. $n = 6$. (**D**) Promotion of anti-PC antibodies to the blood clearance of TIGR4. Blood bacterial loads in *Cd19*$^{-/-}$ mice were counted in the first 12 hours postinfection with 10^6 CFU of the bacteria untreated or pre-opsonized by 5 μg of T15 IgM. $n = 3$ to 6. (**E**) Pivotal role of complement C3 for the blood clearance of TIGR4. Blood bacterial loads in *C3*$^{-/-}$ mice were counted in the first 12 hours postinfection as in (B). $n = 3$ to 6. (**F**) Role of spleen in the clearance of LV pneumococci in liver immunocompromised mice. Blood bacterial loads in KC-specific depletion *Clec4f*-DTR (+DT), control (−DT), and KC-depleted SPX (+DT SPX) mice were compared post intravenous infection with 10^8 CFU of the LV *Spn*14. $n = 3$. Significance was compared by two-way ANOVA test [(B) to (F)]. *$P < 0.05$, ****$P < 0.0001$.

(*17*), KC-deficient mice (*Clec4f*-DTR mice treated with diphtheria toxin, +DT) showed remarkable deficiency in removing *Spn*14 in the first 12 hours post intravenous infection as compared with the untreated mice (−DT) (Fig. 8F). Nevertheless, there was a gradual clearance of the blood *Spn*14 in KC-deficient mice in the first 12 hours, resulting in a 230-fold reduction in blood bacteria compared to the inoculum, but this slow clearance was completely lost after the spleen was surgically removed in DT-treated *Clec4f*-DTR mice (+DT SPX) (Fig. 8F). This result showed that the spleen is a vital backup firewall against encapsulated pneumococci that cannot be cleared by the liver.

DISCUSSION

It has been well documented that humans lacking a functional spleen are highly susceptible to invasive infection by *S. pneumoniae* and other encapsulated bacteria (*21*, *22*); however, it remains largely unknown how the largest immune organ executes its innate immunity against these bacteria. In this study, we have uncovered the dominant role of RP macrophages in the splenic clearance of HV pneumococci by taking advantage of their ability to escape the liver surveillance (*17*, *18*). We've further demonstrated that this organ-specific innate immunity requires opsonization of nAbs targeting the cell wall PC of *S. pneumoniae* and activation of the complement system. While RP macrophages, nAbs, and the complement system are known to contribute to host innate immunity against invasive bacterial infections, this study represents the first mechanistic map of the antibacterial machinery in the spleen (fig. S9).

The spleen is the backup immune organ for the hepatic antibacterial firewall

As represented by the reticuloendothelial system (*12*, *13*), there are a plenty of more recent evidence that both the spleen and liver are important in host defense against bacterial infections (*14*, *25*, *63*–*65*). However, it remains largely undefined how the two organs divide the labor in the clearance of invading bacteria. Our recent studies have defined that the liver KCs capture and kill unencapsulated and many LV encapsulated bacteria with astonishing efficiency in mice once they enter the blood circulation; the spleen is completely dispensable for the clearance of these bacteria (*17*, *18*). This work has shown that the spleen clears encapsulated bacteria that the liver fails to eliminate. On the one hand, the spleen eliminates the liver-resistant bacteria that are naturally refractory to the hepatic firewall. This is manifested by the survival and subsequent growth of the liver-resistant HV serotypes in the blood circulation in the absence of the spleen. On the other hand, the spleen is able to control the blood-borne LV encapsulated bacteria when the hepatic filtration system is compromised. The spleen became essential for clearing the otherwise liver-susceptible LV pneumococci in KC-depleted mice. In such scenarios, the spleen serves as a backup, albeit less efficient, immune organ of the hepatic antibacterial firewall.

In summary, the liver appears to serve as the default organ for removing the "conventional" microorganisms in the bloodstream (e.g., gut microbiota and LV encapsulated bacteria), while the spleen is reserved for dealing with the "emergency" conditions due to invasive infections of the liver-resistant pathogens or the impairment of the hepatic surveillance system. The layback role of the spleen, relative to the liver, in bacterial clearance is consistent with the well-known role of the spleen in sampling microbial antigens in the circulation for B cell activation and antibody production (*20*), which would provide more swift responses to potential future emergency. Technically, the recent availability of the liver-resistant pneumococcal serotypes has enabled us to distinguish the unique contributions of the spleen and liver to bacterial clearance.

RP macrophage is the major immune cell against the liver-resistant pneumococci in the spleen

Despite the importance of the spleen in host defense against microbial infections, the splenic immune cells that execute bacterial clearance are still sketchy and controversial. MZ macrophages bind pneumococcal capsules via the C-type lectin receptor SIGN-R1 (*28*–*31*), which has been suggested to be essential for the clearance of pneumococci in mice (*30*, *31*). In contrast, a more recent study has suggested RP macrophages, instead of MZ macrophages, as the leading phagocytes for phagocytic clearance of virulent *S. pneumoniae* in the spleen (*27*). *Leishmania donovani*–induced expansion of RP macrophages made mice more resistant to serotype-3 HV pneumococci although the parasitic infections also resulted in the simultaneous loss of MZ macrophages; in addition, neutrophils and dendritic cells are dispensable (*27*). A subsequent study has confirmed the role of RP macrophages in capture serotype-2 pneumococci in the spleen but also showed that neutrophils are responsible for killing RP macrophage–trapped bacteria in the spleen (*25*).

This work has provided evidence that RP macrophages are the major immune cells in the spleen that capture and kill the liver-resistant pneumococci in the early phase of septic infection. Our conclusion is supported by the complete loss of pneumococcal clearance in RP macrophage–deficient mice. This phenotype was identified by high CL–mediated RP macrophage depletion and later confirmed by SpiC-dependent genetic deficiency in RP macrophage development. In sharp contrast, parallel experiments targeting MZ and MP macrophages did not yield obvious impact on the splenic clearance of the liver-resistant bacteria. Moreover, we have found that neutrophils play a marginal role in the splenic clearance of virulent pneumococci in the early phase of infection. Splenic neutrophils dramatically increased at 3 to 6 hours postinfection, but depleting neutrophils with 1A8 antibody did not yield notable impact on the eradication of blood-borne pneumococci. The in vivo imaging and flow cytometry data also showed a dominant role of RP macrophages in capturing and killing pneumococci in the spleen. Neutrophils and IMs appear to confer a lower level of antipneumococcal immunity at 12 hours postinfection since Gr1 antibody–treated mice showed noticeable impairment in pneumococcal clearance from the bloodstream. In full agreement with our finding, Gerlini *et al.* (*34*) have shown that splenic macrophages are much more important than neutrophils and IMs in the clearance of pneumococci from the blood circulation.

The tissue resident macrophages shape the spleen- and liver-specific immune functions

Building on our previous studies on the unique role of KCs in liver-specific bacterial clearance (*17*, *18*), this study has clarified the function of RP macrophages in the spleen-specific immunity against the liver-resistant pneumococci, improving our understanding on how the spleen and liver carry the organ-specific antibacterial immunity. The RP macrophages and KCs share several anatomic and functional features (*66*, *67*). In contrast to the intrinsic mobility of certain tissue-resident macrophages (e.g., alveolar macrophage and peritoneal macrophage), both RP macrophages and KCs are immobilized to their niches and directly exposed to blood flow. RP macrophages

and KCs have been well documented as highly phagocytic cells in taking up old/injured erythrocytes (for RP macrophages) and microbes (for KCs). RP macrophages and KCs each represent the most abundant macrophage population in the spleen and liver, respectively. Last, both the macrophage types are characterized by their phagocytic capacities.

However, there are numerous fundamental differences between RP macrophages and KCs, which, to greater or less extents, contribute to the organ-specific immunity. KCs represent approximately 90% of all resident macrophages in the body and are positioned at the gateway of the hepatic portal vein where blood from the gastrointestinal systems gather and pass through the liver sinusoids (*68*). The liver macrophages are also famous for its swift capture of circulating bacteria and other particles (*14*, *25*, *63*–*65*, *69*–*73*). A recent study has shown that KCs positioned near the entry of the portal vein are even more phagocytic than those located at the distal part of the hepatic vasculatures, so-called "commensal-driven immune zonation" (*72*). The anatomic position, exceptional abundance, and enormous phagocytic capacity of KCs suit well with the default immune task of removing potentially abundant and harmful microbes and other particles from the blood circulation. Although RP macrophages are far lower in cell number than KCs, they outnumber the combination of all the other macrophage populations in the spleen of humans and mice (*66*). Moreover, RP macrophages are highly phagocytic as manifested by the effective uptake of aged/damaged erythrocytes or erythrophagocytosis (*74*).

In the light of the existing literature, resident macrophage–specific expression of bacterial pattern–recognition receptors is likely to be a major factor in defining the RP macrophage– and KC-specific activities in clearing blood-borne bacteria. In sharp contrast to the well-documented phagocytic activities of RP macrophage and KCs against bacteria, the receptors that recognize microbial molecules for macrophage phagocytosis are far less understood. However, our recent studies have shown that KCs capture the LV encapsulated bacteria by receptor-mediated recognition of CPSs, as demonstrated by the requirement of asialoglycoprotein receptor (ASGR) for KC capture of serotype-7F and -14 pneumococci in the liver sinusoids (*17*, *18*). While ASGR represents the only known receptor for bacterial capsules on KCs, the liver macrophages also uniquely express the complement receptor CRIg for bacterial phagocytosis, which is virtually not expressed by any other immune cells (*64*, *65*, *69*, *75*, *76*). While there are no existing bacterium-specific receptors on RP macrophages, it is likely that these macrophages also require such receptors for capturing flowing bacteria in the bloodstream. The CD91 and CD163 scavenger receptors have been identified for the uptake of hemopexin-heme complexes and hemoglobin by RP macrophages, respectively (*77*, *78*).

Anti-PC nAbs are essential for the splenic immunity against the liver-resistant *S. pneumoniae*

Since the 1980s, the protective effects of naturally occurred antibodies targeting non-capsular antigens in pneumococcal infection have been documented (*42*, *52*, *54*). NAbs of the T15 idiotype, which recognize the PC moiety in pneumococcal cell wall polysaccharides, have been proved to protect mice from lethal infection by multiple serotypes of pneumococci, with empirical evidence based on the phenotypic observation on blood bacterial clearance and postinfection survival rate (*55*, *79*). In this work, the antibody-null μ*MT* mice and B1 cell–deficient $Cd19^{-/-}$ mice revealed functional impairment in the early control of HV pneumococci, which could be dose-dependently reversed by purified nAbs from murine serum or recombinant monoclonal T15 antibodies. The essentiality of anti-PC nAbs was further confirmed by the in situ 2pSAM illustration of nIgM- and T15 IgM-recovered pneumococcal entrapment in the RP of $Cd19^{-/-}$ mice. Our study has uncovered the cellular basis underlying the protection conferred by anti-PC nAbs, by which RP macrophages capture the circulating HV pneumococci in the spleen, thus maintaining a fundamental level of antipneumococcal immunity in the native host. Nevertheless, the nAb-deficient mice showed lower bacteremia level than that in the asplenic and RP macrophage–depleted mice over the initial phase of infection, which suggests nAb-independent yet unknown immune functions in the spleen.

In agreement with previous studies (*80*–*82*), we observed substantial levels of PC-reactive IgM and IgG antibodies in serum from adult donors. While anti-PC antibodies are commonly present in healthy adults, they are notably absent in infants under 2 months of age and decline dramatically in the elderly (*81*). This deficiency in anti-PC antibodies may partially explain the increased susceptibility of these populations to invasive pneumococcal diseases, highlighting the critical role of these antibodies in host defense.

Our recent work has highlighted that vaccine-elicited anti-capsule antibodies strongly augment the immune clearance of HV pneumococci by liver KCs and sinusoidal endothelial cells, thus providing robust protection (*48*). Moreover, we found that the splenic defense can be bolstered by additional anti-PC antibodies, which could convert the slow bacterial clearance to a rapid elimination and partially protect the host from lethal infection, underscoring the viability of pneumococcal PC as vaccine candidates. Despite the success of current capsule-based pneumococcal vaccines, they do face the limitations in serotype coverage and the challenges of serotype replacement (*83*). Consequently, antibodies targeting the conserved non-capsular antigens offer a compelling strategy for broad-spectrum vaccines that are effective against all serotypes of *S. pneumoniae*. To this end, various pneumococcal surface proteins have been widely explored as vaccine antigens, with several protein-based vaccines being used in clinical trials (*84*). However, there remains interstrain variability in some pneumococcal surface proteins (*85*), which has been reported to promote immune evasion to variant-specific antibodies (*86*). The strictly immutable nature of the pneumococcal cell wall PC makes it a promising antigen for future vaccine development. Nonetheless, ongoing research efforts are imperative to optimize the efficacy of immune clearance mediated by anti-PC antibodies and to explore their full clinical potential.

Complement system is pivotal for the antibacterial immunity in the spleen

The complement system represents an important element of the innate immunity to bacterial infections, including *S. pneumoniae* (*87*). It is not unusual that complement systems played a role in the RP macrophage–dependent pneumococcal clearance. Our findings demonstrate that complement C3 is indispensable for the efficient elimination of HV pneumococci during the early stage of septic infection, acting synergistically with RP macrophages and nAbs to mediate bacterial clearance. Moreover, the monoclonal T15 IgM- or IgG3-opsonized pneumococci cannot be efficiently eliminated in $C3^{-/-}$ mice as compared with the rapid clearance in WT controls. These results indicate the complement system as a pivotal downstream effector mechanism of nAb-driven innate defense in the

spleen. Unexpectedly, the splenic immunity seems to be less dependent on the classical pathway initiated by nAb because the *C1qa*$^{-/-}$ mice held the capacity to eliminate HV pneumococci as the WT controls. Instead, we noticed a severe impairment in bacterial clearance in alternative pathway–deficient *Cfb*$^{-/-}$ mice. Cell wall teichoic acid plays a critical role in complement activation through alternative pathway on the pneumococcal surface (*88*). nIgM binding to PC could result in local clustering of the teichoic acids due to the agglutinating effect of the 10-valent IgM, which in turn accelerates the assembly of the alternative C3 convertase C3bBb and its amplification loop. This may explain why the alternative pathway is more relevant than the classical pathway for splenic clearance of HV *S. pneumoniae*. Although we have established that C3 is required for the nAb-mediated pneumococcal clearance, our in vivo assessment showed dispensable roles of the known complement receptors, including CR1/2, CR3, CR4, and CRIg. How C3-coated pneumococci are destroyed calls for further elucidations.

Limitation of this study

We have investigated the cellular and molecular basis of splenic immunity to HV pneumococci in murine sepsis models, which should be interpreted with caution in the context of human disease. The ubiquity of PC-reactive nAbs in human serum (*81*, *82*, *89*) and their cross protection in mouse models (*52*) strongly suggest the anti-PC antibodies as a conserved immune response to pneumococcal infection across mammalian species. Nonetheless, the translational relevance of our findings needs further exploration.

MATERIALS AND METHODS

Bacterial strains and cultivation

The *S. pneumoniae* strains used in this study are described in table S1. *S. pneumoniae* strains were cultured with Todd-Hewitt broth containing 0.5% yeast extract at 37°C with 5% CO_2, or on tryptic soy agar plates supplemented with 5% defibrinated sheep blood. PC-free *S. pneumoniae* strains were obtained by cultivation of the bacteria in chemically defined medium supplemented with ethanolamine (40 μg/ml) instead of choline as described (*90*).

Mouse lines

The source and strain information of KO mice used in this work is provided in table S2. The *Itgax*$^{-/-}$ (CR4 KO) mice were in-house generated by the CRISPR-Cas9 approach using single-guide RNAs (sgRNAs) (gRNA15312) as listed in table S3. The desirable offsprings were backcrossed with WT C57BL/6J mice for more than seven generations before experimentation. The *Itgam*$^{-/-}$*Itgax*$^{-/-}$ (CR3/CR4 double KO) mouse was generated by CRISPR-Cas9 approach in *Itgam*$^{-/-}$ background using sgRNA targeting *Itgax* locus. The resulting frameshifting mutations in *Itgam* and *Itgax* were confirmed by DNA sequencing.

Septic infection

All animal experiments were performed in female C57BL/6 mice (6 to 8 weeks old) according to the animal protocols approved by the Institutional Animal Care and Use Committee in Tsinghua University (22-ZJR1). Septic infections were carried out by intravenous injection of desirable bacterial CFUs in 100 μl of Ringer's solution as described (*17*). The bacteremia kinetics were determined by retro-orbital bleeding and CFU plating. Bacteria in the spleen and liver were measured by CFU plating of tissue homogenates and presented as CFU per organ. Mouse survival was recorded every day in a 7-day period or at a humane end point (body weight loss >20%).

Splenectomy

Asplenic mice were obtained by surgical removal of the spleen as described (*17*). In brief, the mice were anesthetized with avertin (Sigma-Aldrich) at a dose of 400 mg/kg and meloxicam (Sigma-Aldrich) at a dose of 8 mg/kg before surgery. The peritoneum was opened on the left side to suture spleen pedicle before removing spleen and closing the peritoneum. SHM mice underwent the same procedure without spleen removal. Postoperative animals were allowed to recover for at least 10 days before experiments.

Immunofluorescence imaging of the spleen

Immunofluorescence staining of fixed spleen was carried out as described (*32*). Briefly, the spleens of mice were made into 10-μm frozen sections for confocal immunofluorescence imaging. For analyzing the bacterial capture in the spleen, the mice were intravenously infected with 10^7 CFU of GFP-expressing *S. pneumoniae* 1 hour before preparation of sections. RP, MZ, and MP macrophages were stained with AF647 anti-F4/80, AF488 anti-SIGN-R1, and AF594 anti-CD169, respectively, at 3 μg/ml for 30 min after treatment with 200 μl of blocking buffer [phosphate-buffered saline (PBS) supplemented with 1% bovine serum albumin (BSA)]. Sections were mounted with an antifade mounting media after three washes in PBS. Images were acquired with Leica TCS SP8 confocal microscope using 10×/0.45 NA and 20×/0.80 numerical aperture (NA) HC PL APO objectives. The microscope was equipped with Acousto Optics without filters. Fluorescence signals were detected by photomultiplier tubes and hybrid photo detectors. Three laser excitation wavelengths (488, 585, and 635 nm) were used by white light laser (1.5 mw, Laser kit WLL2, 470 to 670 nm). Representative images were acquired with 200× and 800× magnification at 1024 pixels by 1024 pixels. The RP and MZ of the entire spleen section were photographed by concatenating multiple images at 100× magnification, and the area was calculated by ImageJ (ImageJ 1.47v, National Institutes of Health, USA). Five to 10 random fields of view were examined to calculate the number of captured bacteria in each area. Antibodies used in this study are listed in table S4.

Long-term 3D two-photon imaging of the spleen

Subcellular resolution imaging of the spleen was performed by 2pSAM essentially as described (*39*). Briefly, RP macrophages and neutrophils were stained with 2.5 μg of phycoerythrin (PE) anti-F4/80 and PE-Cy5 anti-Ly6G, respectively, 30 min before intravenous infection with 5×10^6 CFU of GFP-expressing *S. pneumoniae*. The spleen was surgically exposed and fixed by a vacuum apparatus under the lens. The mice were kept in anesthesia using 1.5% of isoflurane. An excitation light from a commercial femtosecond laser (Spectra-Physics InSight X3, Newport) was set at 1000 nm for three-color imaging. The average laser power under the objective (25×/1.05 NA, water immersion, Olympus, XLPLN25XWMP2) was about 30 mW. For detection, a 525-nm filter (MF525-39, Thorlabs) was used for bacteria imaging, a 610-nm filter (ET610/75 m, Chroma) was used for macrophage imaging, and a 670-nm filter (ET670/50 m, Chroma) for the neutrophil imaging. Imaging data were collected at a 30-Hz sampling rate, and 512 pixels–by–512 pixels–by–13 angles scanning was adopted. Before three-dimensional (3D) reconstruction, DeepCAD was used to perform denoising for each angle (*91*),

and a customized denoising model was trained for each channel. The 3D reconstruction was performed as described (*39*).

Bacterial uptake by RP macrophages was visualized by 2pSAM as described (*17*). The splenic RP macrophages were stained by intravenous injection of 2.5 μg PE-Cy5 anti-F4/80 antibodies at 30 min before intravenous inoculation with 10^7 CFU of pHrodo-labeled GFP-expressing *S. pneumoniae*. pHrodo labeling was conducted according to the manufacturer's instructions except for using 0.001 mM pHrodo Red (Invitrogen). Images were acquired at 1 hour postinfection.

Bacterial cell tracking was performed using a deep learning model that integrates the bacterial motility conditions and cellular feature similarity in 2pSAM images to comprehensively reconstruct cell movement trajectories as described (*92*). To reduce interference caused by extraneous bacterial and noise signals, bacteria appearing briefly (less than two frames) were excluded from the data.

Immune cell depletion

MZ/MP macrophages and RP macrophages were selectively depleted by intravenous inoculation with low CL (120 μg per mouse) and high CL (1 mg per mouse) 1 day before infection, respectively, as described (*25*). Antibody-based depletion of neutrophils and IMs was accomplished as described in our previous study (*17*). KCs were removed by intraperitoneal injection of recombinant DT in *Clec4F*-DTR mice 1 day before infection (*93*).

Flow cytometry

Flow cytometry was performed essentially as described (*17*). Total splenocytes were harvested by passing through a 70-μm cell strainer, and red blood cells (RBCs) were lysed by 1 ml of RBC lysis solution. The splenocytes (10^6) were blocked with 50 μl fluorescence-activated cell sorting buffer [PBS with 3% fetal bovine serum (FBS)] containing 1% anti-CD16/32 antibody for 10 min and then stained with antibodies: allophycocyanin (APC)–Cy7 anti-CD45 (1/200), BV605 anti-CD11b (1/500), fluorescein isothiocyanate anti-F4/80 (1/200), AF700 anti-Ly6G (1/500), eFluor 450 anti-Ly6C (1/500), APC anti–SIGN-R1 (1/200), and PE anti-CD169 (1/200) for 20 min. Cell viability was characterized by adding 5 μl of 7-AAD to the samples before analysis. Viable cells were gated as splenic RP macrophages ($CD45^+CD11b^{low}F4/80^+$), MZ macrophages ($CD45^+CD11b^+F4/80^-SIGN\text{-}R1^+$), MP macrophages ($CD45^+CD11b^+F4/80^-CD169^+$), neutrophils ($CD45^+CD11b^+Ly6C^+Ly6G^+$), and IMs ($CD45^+CD11b^+Ly6C^{high}Ly6G^-$). For analyzing the bacterial association with splenic phagocytes, the mice were intravenously infected with 10^7 CFU of GFP-expressing *S. pneumoniae* 30 min before harvesting splenocytes and cells were stained as above recipe except using PE-Cy5 anti-F4/80 and excluding 7-AAD. The information of flow antibodies is listed in table S4.

Purification of nAbs

nIgM and nIgG were purified from normal murine serum using Protein G and Protein L resin (GenScript, China) according to the manufacturer's instructions. Briefly, a total volume of 10 ml of serum was diluted with 10 ml of PBS and incubated with 1 ml of Protein G resin at 4°C for 2 hours. The resin was washed with 5 ml PBS for four times, and bound IgG was eluted with 10 ml of 0.1 M glycine (pH 2.5). The flow-through serum from Protein G columns was further mixed with 1 ml of Protein L resin to purify IgM in a similar manner. Purified IgM and IgG were concentrated by ultracentrifugation using 30-kDa centrifugal filters (Millipore, USA), sterilized by 0.22-μm centrifugal filter (Corning, USA), and quantified by the BCA Assay Kit (Beyotime, China).

Recombinant monoclonal antibody production

Murine monoclonal antibodies (idiotype T15) against PC were generated as described with minor modifications (*94*). The coding sequences of variable region for heavy chain (GenBank accession M16334.1) and light chain (GenBank accession U29423.1) were synthesized according to published sequences (*95*, *96*). The coding sequences of constant region for heavy chains (CH_{IgM}, CH_{IgG3}, CH_{IgG1}), light chain, and J chain were polymerase chain reaction (PCR) amplified using murine spleen cDNA as templates. The full-length spleen cDNA was amplified from the total RNA extracted from mouse spleen by TRIzol reagent (Invitrogen) using Maxima H Minus First Strand cDNA Synthesis Kit (Thermo Fisher Scientific). The DNA fragments were further linked by fusion PCR and cloned into H and L vectors by enzymatic digestions and ligations. The relevant primers and resulting plasmids are listed in tables S3 and S5. The full-length IgG3 and IgM antibodies were produced by cotransfection of the H and L vectors into the human embryonic kidney (HEK) 293 suspension culture cells (Expi293F) and purified with Protein G (IgG) and Protein L (IgM) resin, respectively.

Enzyme-linked immunosorbent assay

Antibody titers of human and murine serum and purified IgG/IgM were quantified by ELISA. Human serum samples were collected from healthy donors with approval by the Tsinghua University Science and Technology Ethics Committee (Medicine) (THU01-20240036). Briefly, antigens in 100 μl of PBS were coated on 96-well plates at indicated concentrations: pneumococcal cells, optical density at 600 nm 0.1; BSA and BSA-PC (10 μg/ml); CPS (10 μg/ml). BSA-PC was produced as reported (*97*). Briefly, 75 mg of cytidine 5′-diphosphocholine (CDPC, Sigma-Aldrich) was oxidized in 2.5 ml of 0.1 M sodium periodate for 20 min before 0.15 ml of 1 M ethylene glycol was added to stop the reaction. BSA (140 mg, Sigma-Aldrich) was dissolved in 5 ml of 0.1 M sodium bicarbonate and incubated with the activated CDPC for 1 hour. After that, 5 ml of 0.5 M sodium borohydride was added, and the mixture was incubated overnight. The resulting solution was buffer-exchanged with PBS by ultracentrifugation. CPS was extracted as described (*17*). Immunoglobulin class and subtype were determined with horseradish peroxidase–conjugated anti-mouse or anti-human IgM and IgG antibodies (EasyBio, Beijing, China).

Construction of antibody receptor–expressing CHO cells

CHO cell lines expressing mouse antibody receptors were constructed as described (*48*). For expression of mouse *Fcmr* and *Fcamr*, the full-length cDNAs of the target mouse genes were amplified from the total RNA isolated from the spleen using TRIzol reagent (Invitrogen) using Maxima H Minus First Strand cDNA Synthesis Kit (Thermo Fisher Scientific) and cloned into pCDH vector with a His_6 tag at the C terminus. The ligation mixtures were transformed into *Escherichia coli* DH5α and selected on LB plates with ampicillin (100 μg/ml). Recombinant plasmids were confirmed by DNA sequencing and extracted using HiPure Plasmid EF Micro Kit (Magen) for subsequent lentiviral transduction. Recombinant plasmids were transfected into HEK293T cells using Lipofectamine 2000 (Invitrogen) together with lentiviral packaging vectors pMD2.G and psPAX2 (gifts from D. Trono, Addgene). The lentiviral particles

were harvested at 48 hours and filtered through 0.45-μm syringe filter unit (Millipore) to remove cell debris. The pCDH-lentivirus was used to infect CHO cells with polybrene (8 μg/ml, Sigma-Aldrich). The transfectants were selected with puromycin (5 μg/ml) for 7 days. The relevant primers and resulting plasmids are listed in tables S3 and S5.

RP macrophage cultivation

Mouse primary RP macrophages were isolated and cultivated as described (*98*). In brief, the splenocytes were harvested by grinding the spleen and resuspended in 5 ml of RPMI 1640 medium. Single cells were obtained by filtering through a 70-μm cell strainer, and RBCs were lysed with RBC lysis solution. Splenocytes from each spleen were resuspended in 10 ml of conditional medium (CM, RPMI 1640 supplemented with 20% L929 cell supernatant and 10% FBS) and cultured in a 10-mm plate at 37°C, 5% CO_2 for 3 days. Nonadherent cells were removed, and the adhered RP macrophages were cultured in CM for another 4 days before use.

In vitro bacterial binding

Bacterial binding to host cells were assessed essentially as described (*17*). CHO transfectants and primary RP macrophages were seeded in 96-well cell culture plates and grown to 90 to 100% confluence (~5×10^4 cells per well). At the time of binding experiments, growth media were replaced with basic F-12 K (CHO cells) or RPMI 1640 (RP macrophages) without serum and antibiotics. For pre-opsonization, every 10^7 CFU of pneumococcal cells were incubated with 20 μg of monoclonal T15 antibody or 50 μl of mouse serum at 37°C for 30 min. Antibody or complement-coated bacteria were suspended in basic F-12 K or RPMI 1640 at a density of 5×10^4 CFU in 50 μl and added into 96-well plates with 50 μl per well, resulting in a multiplicity of infection of 1:1, followed by centrifugation at 500*g* for 5 min to maximize the contact between bacteria and the cells. The mixtures were incubated for 30 min at 37°C with 5% CO_2. The free bacteria were enumerated by CFU plating of the supernatants. The eukaryotic cells were thoroughly washed to remove free bacteria and lysed with 100 μl of ice-cold sterile H_2O to enumerate cell-associated bacteria by CFU plating of the lysates. Bacterial binding was calculated by dividing the cell-associated CFU to the CFU of total bacteria.

Statistical analysis

All experiments presented in this work were repeated at least twice at different times. The data are analyzed and presented as means ± SEM. Statistical analysis was performed using GraphPad Prism software (8.3.1). The levels of statistical significance are defined by *P* values of <0.05 (*), <0.01 (**), <0.001 (***), and <0.0001 (****). Flow cytometry and gene/protein sequence data were analyzed using FlowJo (10.4) and Lasergene (15.0.0) for Macintosh, respectively.

Supplementary Materials

The PDF file includes:

Figs. S1 to S9
Tables S1 to S5
Legends for movies S1 to S5

Other Supplementary Material for this manuscript includes the following:

Movies S1 to S5

REFERENCES AND NOTES

1. GBD 2019 Antimicrobial Resistance Collaborators, Global mortality associated with 33 bacterial pathogens in 2019: A systematic analysis for the Global Burden of Disease Study 2019. *Lancet* **400**, 2221–2248 (2022).
2. H. An, Y. Liu, C. Qian, X. Huang, L. Wang, C. Whitfield, J.-R. Zhang, "Bacterial capsules" in *Molecular Medical Microbiology*, Y.-W. Tang, M. Hindiyeh, D. Liu, A. Salis, P. Spearman, J.-R. Zhang, Eds. (Academic Press, ed. 3, 2024), vol. 1, chap. 5, pp. 69–96.
3. C. Taylor, I. S. Roberts, "The regulation of capsule expression" in *Bacterial Adhesion to Host tissues– Mechanisms and Consequences*, M. Wilson, Ed. (Cambridge Univ. Press, 2002), chap. 5, pp. 115–138.
4. E. J. Brown, H. D. Gresham, "Phagocytosis" in *Fundamental Immunology*, W. E.P., Ed. (Lippincott-Raven Publishers, ed. 6, 2012), pp. 1105–1127.
5. M. H. Nahm, J. Katz, "Immunity to extracellular bacteria" in *Fundamental Immunology*, W. E.P., Ed. (Lippincott-Raven Publishers, ed. 6, 2012), chap. 41, pp. 1001–1015.
6. C. Whitfield, S. S. Wear, C. Sande, Assembly of bacterial capsular polysaccharides and exopolysaccharides. *Annu. Rev. Microbiol.* **74**, 521–543 (2020).
7. S. Manna, J. P. Werren, B. D. Ortika, B. Bellich, C. L. Pell, E. Nikolaou, I. Gjuroski, S. Lo, J. Hinds, O. Tundev, E. M. Dunne, B. D. Gessner, S. D. Bentley, F. M. Russell, E. K. Mulholland, T. Mungun, C. von Mollendorf, P. V. Licciardi, P. Cescutti, N. Ravenscroft, M. Hilty, C. Satzke, *Streptococcus pneumoniae* serotype 33G: Genetic, serological, and structural analysis of a new capsule type. *Microbiol. Spectr.* **12**, e0357923 (2024).
8. D. E. Rogers, Studies on bacteriemia. I. Mechanisms relating to the persistence of bacteriemia in rabbits following the intravenous injection of staphylococci. *J. Exp. Med.* **103**, 713–742 (1956).
9. G. Biozzi, J. G. Howard, B. N. Halpern, C. Stiffel, D. Mouton, The kinetics of blood clearance o isotopically labelled Salmonella entertidis by the reticulo-endothelial system in mice. *Immunology* **3**, 74–89 (1960).
10. E. J. Brown, S. W. Hosea, M. M. Frank, The role of complement in the localization of pneumococci in the splanchnic reticuloendothelial system during experimental bacteremia. *J. Immunol.* **126**, 2230–2235 (1981).
11. Y. Kawai, B. Smedsrod, K. Elvevold, K. Wake, Uptake of lithium carmine by sinusoidal endothelial and Kupffer cells of the rat liver: New insights into the classical vital staining and the reticulo-endothelial system. *Cell Tissue Res.* **292**, 395–410 (1998).
12. L. Aschoff, Das reticulo–endotheliale system in *Ergebnisse der Inneren Medizin und Kinderheilkunde*, (Springer, 1924).
13. R. van Furth, Z. A. Cohn, J. G. Hirsch, J. H. Humphrey, W. G. Spector, H. L. Langevoort, The mononuclear phagocyte system: A new classification of macrophages, monocytes, and their precursor cells. *Bull. World Health Organ.* **46**, 845–852 (1972).
14. C. N. Jenne, P. Kubes, Immune surveillance by the liver. *Nat. Immunol.* **14**, 996–1006 (2013).
15. M. L. Balmer, E. Slack, A. de Gottardi, M. A. Lawson, S. Hapfelmeier, L. Miele, A. Grieco, H. Van Vlierberghe, R. Fahrner, N. Patuto, C. Bernsmeier, F. Ronchi, M. Wyss, D. Stroka, N. Dickgreber, M. H. Heim, K. D. McCoy, A. J. Macpherson, The liver may act as a firewall mediating mutualism between the host and its gut commensal microbiota. *Sci. Transl. Med.* **6**, 237ra266 (2014).
16. K. Wake, Y. Kawai, B. Smedsrod, Re-evaluation of the reticulo-endothelial system. *Ital. J. Anat. Embryol.* **106**, 261–269 (2001).
17. H. An, C. Qian, Y. Huang, J. Li, X. Tian, J. Feng, J. Hu, Y. Fang, F. Jiao, Y. Zeng, X. Huang, X. Meng, X. Liu, X. Lin, Z. Zeng, M. Guilliams, A. Beschin, Y. Chen, Y. Wu, J. Wang, M. R. Oggioni, J. Leong, J. W. Veening, H. Deng, R. Zhang, H. Wang, J. Wu, Y. Cui, J. R. Zhang, Functional vulnerability of liver macrophages to capsules defines virulence of blood-borne bacteria. *J. Exp. Med.* **219**, e20212032 (2022).
18. X. Huang, X. Li, H. An, J. Wang, M. Ding, L. Wang, L. Li, Q. Ji, F. Qu, H. Wang, Y. Xu, X. Lu, Y. He, J. R. Zhang, Capsule type defines the capability of *Klebsiella pneumoniae* in evading Kupffer cell capture in the liver. *PLOS Pathog.* **18**, e1010693 (2022).
19. V. Bronte, M. J. Pittet, The spleen in local and systemic regulation of immunity. *Immunity* **39**, 806–818 (2013).
20. S. M. Lewis, A. Williams, S. C. Eisenbarth, Structure and function of the immune system in the spleen. *Sci. Immunol.* **4**, eaau6085 (2019).
21. J. Chong, P. Jones, D. Spelman, K. Leder, A. C. Cheng, Overwhelming post-splenectomy sepsis in patients with asplenia and hyposplenia: A retrospective cohort study. *Epidemiol. Infect.* **145**, 397–400 (2017).
22. P. D. Sinwar, Overwhelming post splenectomy infection syndrome - review study. *Int. J. Surg.* **12**, 1314–1316 (2014).
23. M. V. Lenti, S. Luu, R. Carsetti, F. Osier, R. Ogwang, O. E. Nnodu, U. Wiedermann, J. Spencer, F. Locatelli, G. R. Corazza, A. Di Sabatino, Asplenia and spleen hypofunction. *Nat. Rev. Dis. Primers.* **8**, 71 (2022).
24. R. E. Mebius, G. Kraal, Structure and function of the spleen. *Nat. Rev. Immunol.* **5**, 606–616 (2005).
25. J. F. Deniset, B. G. Surewaard, W. Y. Lee, P. Kubes, Splenic $Ly6G^{high}$ mature and $Ly6G^{int}$ immature neutrophils contribute to eradication of *S. pneumoniae*. *J. Exp. Med.* **214**, 1333–1350 (2017).

26. F. K. Swirski, M. Nahrendorf, M. Etzrodt, M. Wildgruber, V. Cortez-Retamozo, P. Panizzi, J. L. Figueiredo, R. H. Kohler, A. Chudnovskiy, P. Waterman, E. Aikawa, T. R. Mempel, P. Libby, R. Weissleder, M. J. Pittet, Identification of splenic reservoir monocytes and their deployment to inflammatory sites. *Science* **325**, 612–616 (2009).
27. A. C. Kirby, L. Beattie, A. Maroof, N. van Rooijen, P. M. Kaye, SIGNR1-negative red pulp macrophages protect against acute streptococcal sepsis after Leishmania donovani-induced loss of marginal zone macrophages. *Am. J. Pathol.* **175**, 1107–1115 (2009).
28. Y. S. Kang, J. Y. Kim, S. A. Bruening, M. Pack, A. Charalambous, A. Pritsker, T. M. Moran, J. M. Loeffler, R. M. Steinman, C. G. Park, The C-type lectin SIGN-R1 mediates uptake of the capsular polysaccharide of *Streptococcus pneumoniae* in the marginal zone of mouse spleen. *Proc. Natl. Acad. Sci. U.S.A.* **101**, 215–220 (2004).
29. Y. S. Kang, Y. Do, H. K. Lee, S. H. Park, C. Cheong, R. M. Lynch, J. M. Loeffler, R. M. Steinman, C. G. Park, A dominant complement fixation pathway for pneumococcal polysaccharides initiated by SIGN-R1 interacting with C1q. *Cell* **125**, 47–58 (2006).
30. A. Lanoue, M. R. Clatworthy, P. Smith, S. Green, M. J. Townsend, H. E. Jolin, K. G. Smith, P. G. Fallon, A. N. McKenzie, SIGN-R1 contributes to protection against lethal pneumococcal infection in mice. *J. Exp. Med.* **200**, 1383–1393 (2004).
31. E. A. Koppel, C. W. Wieland, V. C. van den Berg, M. Litjens, S. Florquin, Y. van Kooyk, T. van der Poll, T. B. Geijtenbeek, Specific ICAM-3 grabbing nonintegrin-related 1 (SIGNR1) expressed by marginal zone macrophages is essential for defense against pulmonary *Streptococcus pneumoniae* infection. *Eur. J. Immunol.* **35**, 2962–2969 (2005).
32. G. Ercoli, V. E. Fernandes, W. Y. Chung, J. J. Wanford, S. Thomson, C. D. Bayliss, K. Straatman, P. R. Crocker, A. Dennison, L. Martinez-Pomares, P. W. Andrew, E. R. Moxon, M. R. Oggioni, Intracellular replication of *Streptococcus pneumoniae* inside splenic macrophages serves as a reservoir for septicaemia. *Nat. Microbiol.* **3**, 600–610 (2018).
33. M. Zouali, Y. Richard, Marginal zone B-cells, a gatekeeper of innate immunity. *Front. Immunol.* **2**, 63 (2011).
34. A. Gerlini, L. Colomba, L. Furi, T. Braccini, A. S. Manso, A. Pammolli, B. Wang, A. Vivi, M. Tassini, N. van Rooijen, G. Pozzi, S. Ricci, P. W. Andrew, U. Koedel, E. R. Moxon, M. R. Oggioni, The role of host and microbial factors in the pathogenesis of pneumococcal bacteraemia arising from a single bacterial cell bottleneck. *PLOS Pathog.* **10**, e1004026 (2014).
35. T. L. McGaha, Y. Chen, B. Ravishankar, N. van Rooijen, M. C. Karlsson, Marginal zone macrophages suppress innate and adaptive immunity to apoptotic cells in the spleen. *Blood* **117**, 5403–5412 (2011).
36. M. Kohyama, W. Ise, B. T. Edelson, P. R. Wilker, K. Hildner, C. Mejia, W. A. Frazier, T. L. Murphy, K. M. Murphy, Role for Spi-C in the development of red pulp macrophages and splenic iron homeostasis. *Nature* **457**, 318–321 (2009).
37. N. A-Gonzalez, J. A. Guillen, G. Gallardo, M. Diaz, J. V. de la Rosa, I. H. Hernandez, M. Casanova-Acebes, F. Lopez, C. Tabraue, S. Beceiro, C. Hong, P. C. Lara, M. Andujar, S. Arai, T. Miyazaki, S. Li, A. L. Corbi, P. Tontonoz, A. Hidalgo, A. Castrillo, The nuclear receptor LXRα controls the functional specialization of splenic macrophages. *Nat. Immunol.* **14**, 831–839 (2013).
38. N. V. Serbina, E. G. Pamer, Monocyte emigration from bone marrow during bacterial infection requires signals mediated by chemokine receptor CCR2. *Nat. Immunol.* **7**, 311–317 (2006).
39. Z. Zhao, Y. Zhou, B. Liu, J. He, J. Zhao, Y. Cai, J. Fan, X. Li, Z. Wang, Z. Lu, J. Wu, H. Qi, Q. Dai, Two-photon synthetic aperture microscopy for minimally invasive fast 3D imaging of native subcellular behaviors in deep tissue. *Cell* **186**, 2475–2491.e22 (2023).
40. D. G. Russell, B. C. Vanderven, S. Glennie, H. Mwandumba, R. S. Heyderman, The macrophage marches on its phagosome: Dynamic assays of phagosome function. *Nat. Rev. Immunol.* **9**, 594–600 (2009).
41. B. G. J. Surewaard, P. Kubes, Measurement of bacterial capture and phagosome maturation of Kupffer cells by intravital microscopy. *Methods* **128**, 12–19 (2017).
42. D. E. Briles, M. Nahm, K. Schroer, J. Davie, P. Baker, J. Kearney, R. Barletta, Antiphosphocholine antibodies found in normal mouse serum are protective against intravenous infection with type 3 *Streptococcus pneumoniae*. *J. Exp. Med.* **153**, 694–705 (1981).
43. V. E. Fernandes, G. Ercoli, A. Benard, C. Brandl, H. Fahnenstiel, J. Muller-Winkler, G. F. Weber, P. Denny, L. Nitschke, P. W. Andrew, The B-cell inhibitory receptor CD22 is a major factor in host resistance to *Streptococcus pneumoniae* infection. *PLOS Pathog.* **16**, e1008464 (2020).
44. D. Kitamura, J. Roes, R. Kuhn, K. Rajewsky, A B cell-deficient mouse by targeted disruption of the membrane exon of the immunoglobulin mu chain gene. *Nature* **350**, 423–426 (1991).
45. K. M. Haas, J. C. Poe, D. A. Steeber, T. F. Tedder, B-1a and B-1b cells exhibit distinct developmental requirements and have unique functional roles in innate and adaptive immunity to *S. pneumoniae*. *Immunity* **23**, 7–18 (2005).
46. J. V. Ravetch, S. Bolland, IgG Fc receptors. *Annu. Rev. Immunol.* **19**, 275–290 (2001).
47. D. Ricklin, G. Hajishengallis, K. Yang, J. D. Lambris, Complement: A key system for immune surveillance and homeostasis. *Nat. Immunol.* **11**, 785–797 (2010).
48. J. Wang, H. An, M. Ding, Y. Liu, S. Wang, Q. Jin, Q. Wu, H. Dong, Q. Guo, X. Tian, J. Liu, J. Zhang, T. Zhu, J. Li, Z. Shao, D. E. Briles, J. W. Veening, H. Zheng, L. Zhang, J. R. Zhang, Liver macrophages and sinusoidal endothelial cells execute vaccine-elicited capture of invasive bacteria. *Sci. Transl. Med.* **15**, eade0054 (2023).
49. P. Smith, D. J. DiLillo, S. Bournazos, F. Li, J. V. Ravetch, Mouse model recapitulating human Fcgamma receptor structural and functional diversity. *Proc. Natl. Acad. Sci. U.S.A.* **109**, 6181–6186 (2012).
50. A. Shibuya, N. Sakamoto, Y. Shimizu, K. Shibuya, M. Osawa, T. Hiroyama, H. J. Eyre, G. R. Sutherland, Y. Endo, T. Fujita, T. Miyabayashi, S. Sakano, T. Tsuji, E. Nakayama, J. H. Phillips, L. L. Lanier, H. Nakauchi, Fcα/μ receptor mediates endocytosis of IgM-coated microbes. *Nat. Immunol.* **1**, 441–446 (2000).
51. S. Akula, L. Hellman, The appearance and diversification of receptors for IgM during vertebrate evolution. *Curr. Top. Microbiol. Immunol.* **408**, 1–23 (2017).
52. D. E. Briles, C. Forman, J. C. Horowitz, J. E. Volanakis, W. H. Benjamin Jr., L. S. McDaniel, J. Eldridge, J. Brooks, Antipneumococcal effects of C-reactive protein and monoclonal antibodies to pneumococcal cell wall and capsular antigens. *Infect. Immun.* **57**, 1457–1464 (1989).
53. J. L. Claflin, J. Berry, Genetics of the phosphocholine-specific antibody response to *Streptococcus pneumoniae*. Germ-line but not mutated T15 antibodies are dominantly selected. *J. Immunol.* **141**, 4012–4019 (1988).
54. D. E. Briles, C. Forman, S. Hudak, J. L. Claflin, The effects of idiotype on the ability of IgG1 anti-phosphorylcholine antibodies to protect mice from fatal infection with *Streptococcus pneumoniae*. *Eur. J. Immunol.* **14**, 1027–1030 (1984).
55. D. E. Briles, C. Forman, M. Crain, Mouse antibody to phosphocholine can protect mice from infection with mouse-virulent human isolates of *Streptococcus pneumoniae*. *Infect. Immun.* **60**, 1957–1962 (1992).
56. T. J. Holzer, K. M. Edwards, H. Gewurz, C. Mold, Binding of C-reactive protein to the pneumococcal capsule or cell wall results in differential localization of C3 and stimulation of phagocytosis. *J. Immunol.* **133**, 1424–1430 (1984).
57. M. R. Wessels, P. Butko, M. Ma, H. B. Warren, A. L. Lage, M. C. Carroll, Studies of group B streptococcal infection in mice deficient in complement component C3 or C4 demonstrate an essential role for complement in both innate and acquired immunity. *Proc. Natl. Acad. Sci. U.S.A.* **92**, 11490–11494 (1995).
58. J. S. Brown, T. Hussell, S. M. Gilliland, D. W. Holden, J. C. Paton, M. R. Ehrenstein, M. J. Walport, M. Botto, The classical pathway is the dominant complement pathway required for innate immunity to *Streptococcus pneumoniae* infection in mice. *Proc. Natl. Acad. Sci. U.S.A.* **99**, 16969–16974 (2002).
59. V. M. Holers, Complement and its receptors: New insights into human disease. *Annu. Rev. Immunol.* **32**, 433–459 (2014).
60. J. Yother, C. Forman, B. M. Gray, D. E. Briles, Protection of mice from infection with *Streptococcus pneumoniae* by anti-phosphocholine antibody. *Infect. Immun.* **36**, 184–188 (1982).
61. M. G. Foreman, D. M. Mannino, M. Moss, Cirrhosis as a risk factor for sepsis and death: Analysis of the national hospital discharge survey. *Chest* **124**, 1016–1020 (2003).
62. A. Ashare, C. Stanford, P. Hancock, D. Stark, K. Lilli, E. Birrer, A. Nymon, K. C. Doerschug, G. W. Hunninghake, Chronic liver disease impairs bacterial clearance in a human model of induced bacteremia. *Clin. Transl. Sci.* **2**, 199–205 (2009).
63. C. H. Wong, C. N. Jenne, B. Petri, N. L. Chrobok, P. Kubes, Nucleation of platelets with blood-borne pathogens on Kupffer cells precedes other innate immunity and contributes to bacterial clearance. *Nat. Immunol.* **14**, 785–792 (2013).
64. S. P. Broadley, A. Plaumann, R. Coletti, C. Lehmann, A. Wanisch, A. Seidlmeier, K. Esser, S. Luo, P. C. Ramer, S. Massberg, D. H. Busch, M. van Lookeren Campagne, A. Verschoor, Dual-track clearance of circulating bacteria balances rapid restoration of blood sterility with induction of adaptive immunity. *Cell Host Microbe* **20**, 36–48 (2016).
65. Z. Zeng, B. G. Surewaard, C. H. Wong, J. A. Geoghegan, C. N. Jenne, P. Kubes, CRIg Functions as a macrophage pattern recognition receptor to directly bind and capture blood-borne gram-positive bacteria. *Cell Host Microbe* **20**, 99–106 (2016).
66. D. Kurotaki, T. Uede, T. Tamura, Functions and development of red pulp macrophages. *Microbiol. Immunol.* **59**, 55–62 (2015).
67. O. Krenkel, F. Tacke, Liver macrophages in tissue homeostasis and disease. *Nat. Rev. Immunol.* **17**, 306–321 (2017).
68. M. Bilzer, F. Roggel, A. L. Gerbes, Role of Kupffer cells in host defense and liver disease. *Liver Int.* **26**, 1175–1186 (2006).
69. K. Y. Helmy, K. J. Katschke Jr., N. N. Gorgani, N. M. Kljavin, J. M. Elliott, L. Diehl, S. J. Scales, N. Ghilardi, M. van Lookeren Campagne, CRIg: A macrophage complement receptor required for phagocytosis of circulating pathogens. *Cell* **124**, 915–927 (2006).
70. W. Y. Lee, T. J. Moriarty, C. H. Wong, H. Zhou, R. M. Strieter, N. van Rooijen, G. Chaconas, P. Kubes, An intravascular immune response to *Borrelia burgdorferi* involves Kupffer cells and iNKT cells. *Nat. Immunol.* **11**, 295–302 (2010).
71. B. G. Surewaard, J. F. Deniset, F. J. Zemp, M. Amrein, M. Otto, J. Conly, A. Omri, R. M. Yates, P. Kubes, Identification and treatment of the *Staphylococcus aureus* reservoir in vivo. *J. Exp. Med.* **213**, 1141–1151 (2016).

72. A. Gola, M. G. Dorrington, E. Speranza, C. Sala, R. M. Shih, A. J. Radtke, H. S. Wong, A. P. Baptista, J. M. Hernandez, G. Castellani, I. D. C. Fraser, R. N. Germain, Commensal-driven immune zonation of the liver promotes host defence. *Nature* **589**, 131–136 (2021).
73. D. L. Sun, P. Sun, H. M. Li, M. S. Zhang, G. G. Liu, A. B. Strickland, Y. L. Chen, Y. Fu, J. Xu, M. Yosri, Y. C. Nan, H. Zhou, X. Q. Zhang, M. Q. Shi, Fungal dissemination is limited by liver macrophage filtration of the blood. *Nat. Commun.* **10**, 4566 (2019).
74. D. Bratosin, J. Mazurier, J. P. Tissier, J. Estaquier, J. J. Huart, J. C. Ameisen, D. Aminoff, J. Montreuil, Cellular and molecular mechanisms of senescent erythrocyte phagocytosis by macrophages. A review. *Biochimie* **80**, 173–195 (1998).
75. Y. Duan, H. Chu, K. Brandl, L. Jiang, S. Zeng, N. Meshgin, E. Papachristoforou, J. Argemi, B. G. Mendes, Y. Wang, H. Su, W. Sun, C. Llorente, T. Hendrikx, X. Liu, M. Hosseini, T. Kisseleva, D. A. Brenner, R. Bataller, P. Ramachandran, M. Karin, W. Fu, B. Schnabl, CRIg on liver macrophages clears pathobionts and protects against alcoholic liver disease. *Nat. Commun.* **12**, 7172 (2021).
76. G. Liu, Y. Fu, M. Yosri, Y. Chen, P. Sun, J. Xu, M. Zhang, D. Sun, A. B. Strickland, Z. B. Mackey, M. Shi, CRIg plays an essential role in intravascular clearance of bloodborne parasites by interacting with complement. *Proc. Natl. Acad. Sci. U.S.A.* **116**, 24214–24220 (2019).
77. V. Hvidberg, M. B. Maniecki, C. Jacobsen, P. Hojrup, H. J. Moller, S. K. Moestrup, Identification of the receptor scavenging hemopexin-heme complexes. *Blood* **106**, 2572–2579 (2005).
78. M. Kristiansen, J. H. Graversen, C. Jacobsen, O. Sonne, H. J. Hoffman, S. K. Law, S. K. Moestrup, Identification of the haemoglobin scavenger receptor. *Nature* **409**, 198–201 (2001).
79. M. K. McNamara, R. E. Ward, H. Kohler, Monoclonal idiotope vaccine against *Streptococcus pneumoniae* infection. *Science* **226**, 1325–1326 (1984).
80. M. G. Scott, D. E. Briles, P. G. Shackelford, D. S. Smith, M. H. Nahm, Human antibodies to phosphocholine. IgG anti-PC antibodies express restricted numbers of V and C regions. *J. Immunol.* **138**, 3325–3331 (1987).
81. D. E. Briles, G. Scott, B. Gray, M. J. Crain, M. Blaese, M. Nahm, V. Scott, P. Haber, Naturally occurring antibodies to phosphocholine as a potential index of antibody responsiveness to polysaccharides. *J Infect Dis* **155**, 1307–1314 (1987).
82. S. Nishinarita, S. Sawada, T. Horie, Phosphorylcholine antibodies in pulmonary infection. *Med. Microbiol. Immunol.* **179**, 205–214 (1990).
83. S. W. Lo, R. A. Gladstone, A. J. van Tonder, J. A. Lees, M. du Plessis, R. Benisty, N. Givon-Lavi, P. A. Hawkins, J. E. Cornick, B. Kwambana-Adams, P. Y. Law, P. L. Ho, M. Antonio, D. B. Everett, R. Dagan, A. von Gottberg, K. P. Klugman, L. McGee, R. F. Breiman, S. D. Bentley, Global Pneumococcal Sequencing Consortium, Pneumococcal lineages associated with serotype replacement and antibiotic resistance in childhood invasive pneumococcal disease in the post-PCV13 era: An international whole-genome sequencing study. *Lancet Infect. Dis.* **19**, 759–769 (2019).
84. S. Li, H. Liang, S. H. Zhao, X. Y. Yang, Z. Guo, Recent progress in pneumococcal protein vaccines. *Front. Immunol.* **14**, 1278346 (2023).
85. W. D. Waltman, L. S. McDaniel, B. M. Gray, D. E. Briles, Variation in the molecular weight of PspA (pneumococcal surface protein A) among *Streptococcus pneumoniae*. *Microb. Pathog.* **8**, 61–69 (1990).
86. M. Georgieva, L. Kagedan, Y. J. Lu, C. M. Thompson, M. Lipsitch, Antigenic variation in *Streptococcus pneumoniae* PspC promotes immune escape in the presence of variant-specific immunity. *MBio* **9**, e00264-18 (2018).
87. E. Gil, M. Noursadeghi, J. S. Brown, *Streptococcus pneumoniae* interactions with the complement system. *Front. Cell. Infect. Microbiol.* **12**, 929483 (2022).
88. J. A. Winkelstein, A. Tomasz, Activation of the alternative complement pathway by pneumococcal cell wall teichoic acid. *J. Immunol.* **120**, 174–178 (1978).
89. R. Fiskesund, J. Steen, K. Amara, F. Murray, A. Szwajda, A. Liu, I. Douagi, V. Malmstrom, J. Frostegard, Naturally occurring human phosphorylcholine antibodies are predominantly products of affinity-matured B cells in the adult. *J. Immunol.* **192**, 4551–4559 (2014).
90. A. Tomasz, M. Westphal, Abnormal autolytic enzyme in a pneumococcus with altered teichoic acid composition. *Proc. Natl. Acad. Sci. U.S.A.* **68**, 2627–2630 (1971).
91. X. Li, Y. Li, Y. Zhou, J. Wu, Z. Zhao, J. Fan, F. Deng, Z. Wu, G. Xiao, J. He, Y. Zhang, G. Zhang, X. Hu, X. Chen, Y. Zhang, H. Qiao, H. Xie, Y. Li, H. Wang, L. Fang, Q. Dai, Real-time denoising enables high-sensitivity fluorescence time-lapse imaging beyond the shot-noise limit. *Nat. Biotechnol.* **41**, 282–292 (2023).
92. A. Santella, Z. Du, Z. Bao, A semi-local neighborhood-based framework for probabilistic cell lineage tracing. *BMC Bioinformatics* **15**, 217 (2014).
93. C. L. Scott, F. Zheng, P. De Baetselier, L. Martens, Y. Saeys, S. De Prijck, S. Lippens, C. Abels, S. Schoonooghe, G. Raes, N. Devoogdt, B. N. Lambrecht, A. Beschin, M. Guilliams, Bone marrow-derived monocytes give rise to self-renewing and fully differentiated Kupffer cells. *Nat. Commun.* **7**, 10321 (2016).
94. Q. Liang, Y. Wang, S. Zhang, J. Sun, W. Sun, J. Li, Y. Liu, M. Li, L. Cheng, Y. Jiang, R. Wang, R. Zhang, Z. Yang, Y. Ren, P. Chen, P. Gao, H. Yan, Z. Zhang, Q. Zhang, X. Shi, J. Wang, W. Liu, X. Wang, B. Ying, J. Zhao, H. Qi, L. Zhang, RBD trimer mRNA vaccine elicits broad and protective immune responses against SARS-CoV-2 variants. *iScience* **25**, 104043 (2022).
95. A. M. Giusti, N. C. Chien, D. J. Zack, S. U. Shin, M. D. Scharff, Somatic diversification of S107 from an antiphosphocholine to an anti-DNA autoantibody is due to a single base change in its heavy chain variable region. *Proc. Natl. Acad. Sci. U.S.A.* **84**, 2926–2930 (1987).
96. W. X. Guo, A. M. Burger, R. T. Fischer, D. G. Sieckmann, D. L. Longo, J. J. Kenny, Sequence changes at the V-D junction of the VH1 heavy chain of anti-phosphocholine antibodies alter binding to and protection against *Streptococcus pneumoniae*. *Int. Immunol.* **9**, 665–677 (1997).
97. P. D. Eckersall, J. G. Conner, H. Parton, Conjugation of Cytidine-5′-diphosphocholine to bovine serum-albumin in the development of an enzyme-linked immunosorbent-assay for canine C-reactive protein. *Biochem. Soc. Trans.* **17**, 414–414 (1989).
98. A. Alatery, S. Basta, An efficient culture method for generating large quantities of mature mouse splenic macrophages. *J. Immunol. Methods* **338**, 47–57 (2008).

Acknowledgments: We thank A. Beschin and M. Guilliams for providing the *Clec4F*-DTR mice, M. Haldar for providing the *Spic*$^{-/-}$ mice, J. Ravetch for providing the *Fcgr1/2b/3/4*$^{-/-}$ mice, and Genentech for providing the *Vsig4*$^{-/-}$ mice. We thank the Tsinghua research platforms for assistance in animal experimentation (Laboratory Animal Research Center), flow cytometry (Center for Biomedical Analysis), IVM imaging (Center for Cell Biology), and protein mass spectrometry (Center for Proteomics). **Funding:** This work was supported by the National Key R&D Program of China to H.A. and J.-R.Z. (2023YFC2308003 and 2023YFC2306300), the National Natural Science Foundation of China to J.-R.Z. (82330071), the High-Grade, Precision and Advanced University Discipline Construction Project of Beijing to H.A. (BMU2024GJJXK008), and the Peking University Medicine Sailing Program for Young Scholars' Scientific & Technological Innovation and the Fundamental Research Funds for the Central Universities to H.A. (BMU2024YFJHPY011). **Author contributions:** Conceptualization: H.A., Y.H., and J.-R.Z. Data curation: Z.Z., K.L., Q.D., and J.-R.Z. Formal analysis: H.A., Y.H., Z.Z., J.M., H.Z., and J.-R.Z. Funding acquisition: H.A. and J.-R.Z. Investigation: H.A., Y.H., Z.Z., K.L., J.M., X.H., X.T., J.W., Q.D., and J.-R.Z. Methodology: H.A., Y.H., Z.Z., K.L., J.W., and J.-R.Z. Project administration: H.A., Q.D., and J.-R.Z. Resource: K.L., H.Z., Q.D., and J.-R.Z. Software: Z.Z. and H.Z. Supervision: H.A., K.L., and J.-R.Z. Validation: H.A., Y.H., Z.Z., K.L., J.M., Q.D., and J.-R.Z. Visualization: H.A., Y.H., Z.Z., K.L., H.Z., and J.-R.Z. Writing—original draft: H.A. and J.-R.Z. Writing—review and editing: H.A., Y.H., Z.Z., X.T., Q.D., and J.-R.Z. **Competing interests:** The authors declare that they have no competing interests. **Data and materials availability:** All data needed to evaluate the conclusions in the paper are present in the paper and/or the Supplementary Materials.

Submitted 1 June 2024
Accepted 5 February 2025
Published 12 March 2025
10.1126/sciadv.adq6399